

Reply to Reviewer

Thank you for reviewing our paper.

General comments:

1. Throughout the paper, the expression “drawdown” is used when what the authors really mean is “negative anomalies”.

“Drawdown” refers to the variation amplitude in the seasonal cycle that mostly resulted from strong plants activity. We will clarify this point in the revised paper.

2. Additionally, the reader might be lead to the somewhat implicit conclusion that XCO₂ can’t serve as a constraint on surface fluxes, but this might be an artifact of the multimonth averaging that is used in the analysis in later sections. At least some discussion of the ability of models such as CT to capture transient features needs to be put forth, because these transient spatial gradients could indeed be attributed to fluxes given sufficient accuracy and adequate transport modeling, as has been shown in numerous OSSEs (Liu et al [2014], Miller et al [2007], Rayner and O’Brien [2001], to name just a few). Connecting the analysis in this paper to those earlier studies is critical to readers trying to assess the conclusions of inversion work with OCO-2 and GOSAT.

We agree with the reviewer that transient spatial gradients could indeed be attributed to fluxes. The ability to capture transient feature is important criteria for modeling performance. Transient features, for example, the seasonal cycle, are generally easier to model since the signals are much larger compared with annual average. However, very small biases in seasonal cycle can still cause drastically biased annual fluxes and unrealistic compensating fluxes. The ability to capture transient features and perfect transport in modelling are not enough. We think it is critical to reduce biases in measurements as inputs for inversions. Previous study by Masarie et al. (2011) had evaluated the impact of CO₂ measurement bias on CarbonTracker flux estimates and found that 1 ppm bias at one site, the Park Fall ,Wisconsin (LEF site in our study), can cause 68 Tg C/yr bias in flux estimate for

Temperate North America (~ 10% of the estimated North American annual terrestrial uptake). Flux estimate errors are also found in Europe and boreal Eurasia to compensate for the errors in North America.

Whether or not the column CO₂ can serve as a good constraint on surface fluxes really depends on the biases in column CO₂ retrievals. High accuracy is needed from column CO₂ product to be useful to constrain surface fluxes because column CO₂ is a total column average, thus it is not as sensitive to surface fluxes as surface measurements. For example, a simple mass balance argument shows that all U.S. CO₂ emissions from fossil fuel burning (~1.4 Pg yr⁻¹) create a total column enhancement of only **0.6 ppm** on average in air parcels over the East Coast compared to the West Coast and Gulf Coast if we assume a residence time of the emissions of 5 days to pass the contiguous U.S. (~8×10¹² m²). From the noise to signal ratio perspective, it is important to have high accuracy in column CO₂ products. Considering current state of biases in remote sensing products, we think extensive works are needed to reduce biases. This can be done given enough well-calibrated surface measurements and vertical profiles.

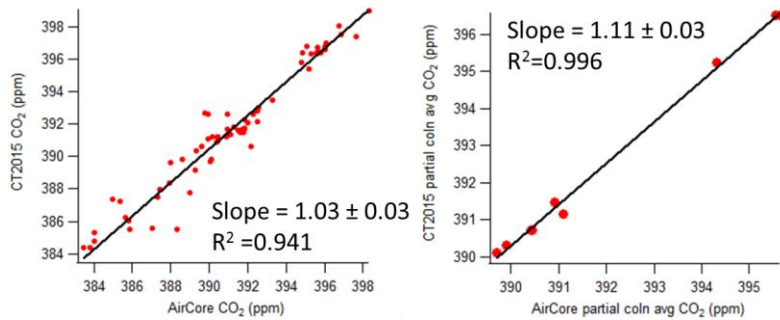
Our study provides an approach to check whether column CO₂ retrievals are satisfying the high accuracy requirement on some levels. Since spatial gradient is the core of deriving reliable regional fluxes, we look into the spatial gradient in long-term multimonth averages, which should be easier for models and column CO₂ products to achieve compared with some short-term metrics (e.g. diurnal cycles).

Specific comments:

1. Figure 2: Are there statistics of goodness of fit? These two examples may not be representative.

We have 9 independent AirCore profiles during study period, which are all sampled nearby CAR and SGP sites. That's why we show one sample from each site. We will clarify this point in the revised paper. The following figures show AirCore vs CT2015 modelled CO₂ above

330hPa. The left panel shows direct point to point comparisons from all 9 profiles at the vertical levels of CT2015; the right panel shows partial column (0- 330hpa) averages. Due to the limited amount of AirCore profiles, we prefer not to put too much discussion of estimate uncertainty in our paper. In addition, the upper 1/3 of the atmosphere is not important when we are looking at long-term averaged spatial gradients in total column because there is little spatial variability in the upper atmosphere. We can see the fit is generally good even when we are comparing at profile by profile basis without temporal averaging.



- Line 207: Can you explain the word “random” here? If all of the profiles are given the same weight in the sampling distribution, then this isn’t really a measure of uncertainty, but rather a weighted standard deviation that would be extremely sensitive to the 100 particles you selected. If there were a “prior” uncertainty placed on each profile, how was that done?

‘random’ means all of the profiles are given the same weight in the Monte Carlo resampling, and the resulting 100 column averages values have a relatively large range since this value are sensitive to the combination of the profiles. That is what we want to use to represent the uncertainty, to account for the atmospheric variability without assuming a giving distribution of the vertical profiles. A ‘prior’ uncertainty is likely to represent mostly the measurement uncertainty, which is too small without fully consider the atmospheric variability.

3. Line 216: There is also some increase due to the shallow PBL alone. It would be good to know what fraction is from the enhancement is due just to boundary layer dynamics. Similarly for the summer.

We agree with the reviewer. However, putting a number on the fractions of enhancement from either changes of PBL or flux requires model with good PBL dynamics and reasonable flux estimates. Good PBL simulations are still very challenging for models. We think it is beyond the scope of this study.

4. Line 228: The PBL height is different at different locations, and through different seasons. How much is the chosen division of the atmosphere mis-attributing boundary layer into the free troposphere, and vice versa? This might be a small detail, but it does impact the conclusions later about the seasonal strength of sources and sinks by region.

For the < 2 km measurements, we believe both PBL and fluxes are important driving factors for the signals we observe. By choose a giving height (2 km), we have removed some of the PBL effect by compensating the PBL with some free-troposphere air. If we use actual temporally changing PBL height as threshold, we will see stronger influences of PBL in wintertime as the CO₂ levels in shallow PBL are even higher compared to our approach. At this moment, we cannot estimate the total influence of PBL and completely remove it without using a model, which may also have big uncertainty in PBL estimates. Our study does not focus on the discussion of the actual number of the fluxes.

5. Line 257: "The SE region also demonstrates a less pronounced seasonal cycle with weaker summer drawdown compared with other northern regions, which may due to the sea-breeze influence in summer within PBL." Is this a statement about the actual impact of the sea breeze on the fluxes, or is it an assertion that we can't interpret the column due to the meteorology?

We state the possible impact of sea breeze on the data and the gradient without implying the interpretation of column data. Given a model with good performance on sea-land

breeze and sufficient accuracy in column CO₂, we should be able to interpret the column data that influenced by sea-land breeze. The message here is that we should take into account of the sea-land breeze effect when interpreting the data.

6. Figure 4: It would be useful to have a fifth panel that shows full column XCO₂ with the CT extension here, to re-inforce the assertion on line 249-250 about the information lost by considering the total column.

It is presented in Figure 7c. We will point the reader to Figure 7c in this part of the description.

7. Figure 9a: The multi-month average XCO₂ gradients can easily miss transient features that could, in theory, be well captured by a regional transport model having spatial resolution that is sufficient to capture synoptic features such as fronts. These features could be attributed to fluxes under this assumption, provided biases are small. That doesn't discount this analysis, but it does imply the need to make assertions about the constraint of XCO₂ on surface fluxes.

The purpose of Figure 9a is to show that CT2015 can compare well with XCO₂ from aircrafts data at this temporally averaged scale, and we should expect a smooth spatial gradient pattern at this temporal scale. This is another baseline to evaluate the performances of models and column CO₂ retrievals, in additional to transient features. Please also see our responses in General Comment.

8. Fig 9b: This vertically averaged wind vector plot doesn't really match the spatial gradient well, in some cases actually being perpendicular to the field. It would make more sense to use the potential temperature at 700mb, as did Keppel-Aleks et al in the reference you cite. Alternately, the 500mb geopotential height is a commonly used field for synoptic scale transport in NWP.

We agree with the review that potential temperature and geopotential height patterns can better match with CO₂ spatial gradient; however, these terms are less straight forward when we interpretation the transport and point to the source regions. We think the wind pattern is sufficient to show the upwind locations we discuss in this study.

9. Figure 10: Can you show the same plots, but for the partial columns that are depicted in Figure 9c and d? That would really drive home the point about transport versus local fluxes.

We will provide these figures in the revised paper:

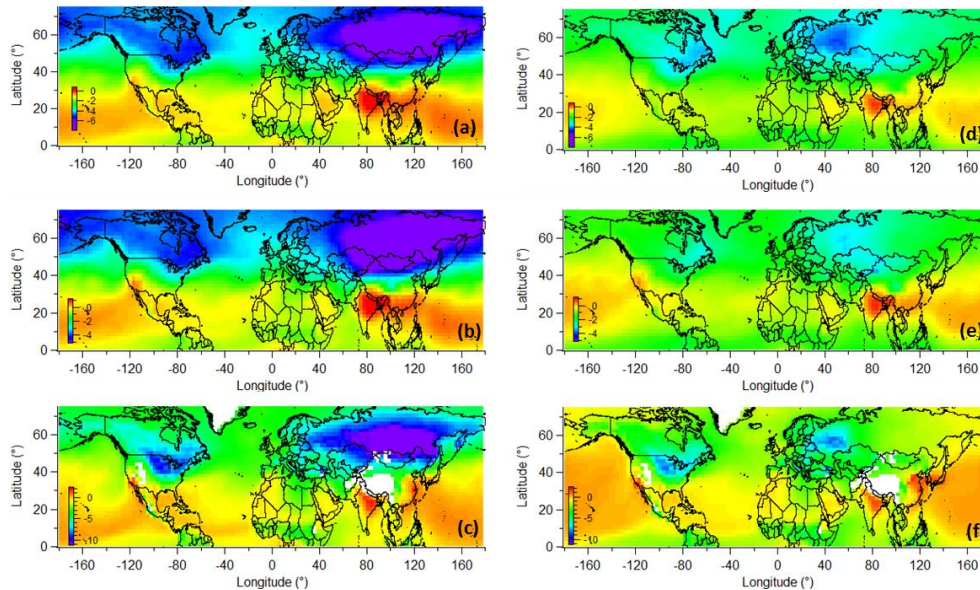


Figure. Total and partial column ΔXCO_2 from Carbon Tracker control (left panels: (a), (b), and (c)) and masked (right panels, (d), (e), and (f). Eurasian boreal flux is masked) runs for 2012 June-August ($3^\circ \times 2^\circ$ spatial resolution). MLO trend from each individual scenario is removed before the ΔXCO_2 calculation. (a) and (d) show total column averages. (b) and (e) show partial column averages for free troposphere (800 hPa to 330 hPa). (c) and (f) show partial column averages for lower troposphere (below 800 hPa). (a) and (d) use the same color scale as in Fig. 9a., which reflects maximum 6 ppm gradient. Color scale in (b) and (e)

also shows maximum 6 ppm gradients for comparison with (a) and (d); however, the actual values are different. Color scales in (c) and (f) are larger to reflect large spatial gradients in lower troposphere.

10. Discussion of Reuter et al [2014]: Is it possible that the differences are due to the manner in which the anomalies are computed? Or are you asserting that the gradients are due to satellite measurement bias? Stating that they "should not be used" needs a bit more justification here.

We don't think the manner in which the anomalies are computed is the reason for the unrealistic gradient. According to their description, the long-term trend has been removed when computed the anomalies, just as in our study. They use 8-year summertime data, which should provide enough data for a reasonable averaged pattern. Thus the quality of the retrievals is likely the reason for an unrealistic pattern. Since the spatial gradient is the core of inversion study to estimate fluxes, it is critical for the input data to have good spatial gradients. We will add in more discussion in the revised paper.

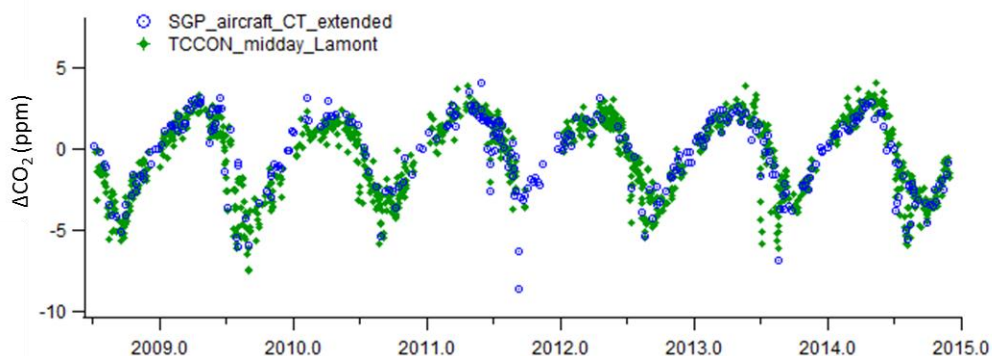
Reply to Reviewer:

Thank you for reviewing our paper.

General comments:

My major comment is that this paper is begging for a direct comparison between the aircraft-derived XCO₂ quantity and those measured via remote sensing at coincident TCCON stations. The obvious two sites would be at LEF (Park Falls) and SGP (Lamont) for which TCCON measurements exist since 2004 and 2008, respectively. There is also a TCCON station at ETL, but it has been measuring for less than one year and would therefore be less useful for this study. It would significantly strengthen this paper if the authors could show that their method of integrating the aircraft and extending the profile into the stratosphere with CT compares well with, or improves upon, the total column measurements from TCCON. The authors could average the TCCON XCO₂ within an hour or so of the aircraft profile times for an apples-to-apples comparison. They could then use the remaining TCCON data (or at least the near-noon data) to investigate any biases or missing information caused by the relatively infrequent aircraft measurements. As part of this comparison, a more rigorous error analysis of the aircraft-derived XCO₂ would be necessary.

We agree with the reviewer that it will be interesting to compare TCCON with aircraft + CT based total column CO₂. The following figure can give us some ideas about this comparison. TCCON values in this figure are daily averages computed from mid-day data (10 to 15 LST). Outliers in TCCON data are filtered out, by using 3.S.D threshold of residuals (with iteration) from a quadratic fit on data for each day.



TCCON Data DOI [10.14291/tcon.ggg2014.lamont01.R0/1149159](https://doi.org/10.14291/tcon.ggg2014.lamont01.R0/1149159)

TCCON reference Wunch, D., G. C. Toon, J.-F. L. Blavier, R. A. Washenfelder, J. Notholt, B. J. Connor, D. W. T. Griffith, V. Sherlock, and P. O. Wennberg (2011), The total carbon column

observing network, *Philosophical Transactions of the Royal Society - Series A: Mathematical, Physical and Engineering Sciences*, 369(1943), 2087-2112, doi:10.1098/rsta.2010.0240. Available from: <http://dx.doi.org/10.1098/rsta.2010.0240>

However, it is not an apple-to-apple comparison between our aircraft-based column CO₂ and TCCON. The sampling time and location are different. Aircraft sampling typically takes ~ 30 min to get the whole profile through downward spiral, mostly within 0.1° of the site location. For TCCON that sampling the whole column instantly at an angle, the actual sampling location, especially at high altitudes, may be far away from our aircraft inlets even though the distance on the ground is much smaller. Mismatches caused by both sampling time and location should be examined carefully if we want answers for accuracy, which should be the topic of another in-depth study. In addition, the aircraft and tower measurements are calibrated on WMO scale; however, direct calibrations of remote sensing instruments are not available. It makes more sense to compare TCCON against calibrated measurements for accuracy instead of the other way around. Our study focuses on the long-term mean spatial patterns of column CO₂ over North America and the influence of large-scale transport; we don't think analysis on two individual TCCON sites can provide extra information regarding to our goal. Previous study by Keppel-Aleks et al. (2012) already provides analysis on TCCON data and meridional spatial patterns.

Specific comments:

1. L19: What does a “stronger summer drawdown” mean? Larger amplitude? Lower minimum?

“Drawdown” refers to the variation amplitudes in the seasonal CO₂ signals that mostly resulted from strong plants activity. We clarify this point in the revised paper.

2. L20: This sentence is contradicted by the conclusions:

“The spatial gradients of total column XCO₂ across North America mainly reflect largescale circulation patterns rather than regional surface sources and sinks.”

Conclusions:

“By comparing the spatial gradients of XCO₂ with wind vectors across North America, we find that total column XCO₂ patterns are equally affected by large-scale circulation patterns as by regional surface sources and sinks.”

Your paper seems to corroborate the sentence in your conclusions and not your abstract.

Please modify the abstract accordingly.

We do not mean that local fluxes have no influence on long-term averaged column CO₂ spatial pattern. But the major contributor is transport, instead of surface flux. We have results from CT experiments showing that 50% of North-South gradient are due to Eurasia flux, which is stated in both abstract and conclusion parts. Since Eurasia flux is not the only transport signals we observed (upwind Canadian region is likely contribute to transport signal too), we actually expected larger than 50% transport influence in total. We will clarify the statement in both abstract and conclusion.

3. L55: in-situ observations are sparse in global and regional coverage, and, with the exception of AirCore measurements are limited in vertical extent - most cannot measure more than 80% of the atmospheric mass.

We agree with the reviewer that aircraft measurements have vertical limitations. However, we should also acknowledge that most of the flux signals reside in the lower part of the atmosphere. There is little spatial variation of atmospheric CO₂ in the stratosphere over mid-latitude region (Andrews et al., 2001). Thus this part of the atmosphere has little contribution to the spatial patterns of total column CO₂ that are used to retrieve surface sources and sinks.

(Citation: Andrews, A., Boering, K., Daube, B., Wofsy, S., Loewenstein, M., Jost, H., Podolske, J., Webster, C., Herman, R., Scott, D., et al.: Mean ages of stratospheric air derived from in situ observations of CO₂, CH₄, and N₂O, *J. Geophys. Res. Atmos.*, 106, 32295–32314, 2001)

4. L73: What are the uncertainties of total column XCO₂ calculated from in situ measurements? According to Wunch et al. 2010, given the lack of measurements above the aircraft ceiling, the total column aircraft uncertainty is 0.4 ppm, which is similar to the TCCON measurement uncertainty. I would expect the errors for the profiles discussed in this paper to have larger uncertainties, since the altitude coverage for the NOAA flights is significantly smaller than the profiles used in the Wunch et al., 2010 paper.

We have provided the uncertainty in partial column CO₂ derived from tower and aircraft measurements in SI, figure S4, which ranges from 0.12 to 0.96 ppm with average value of 0.32 ppm over all eight regions for long-term monthly averaged values (uncertainty in summer months are higher). Uncertainty in vertical profile mainly reflects atmospheric variability instead of just instrument errors. In our study, several regions have more than one aircraft sites. When we are averaging over those sites over a total of 11-year vertical profiles, the uncertainty goes down since we have reduced atmospheric variability significantly. The uncertainty in Wunch et al.,2010 is based on individual profile without long time averaging, thus it is not the same as in our study .

We cannot properly assign an exact number as the uncertainty for the top 1/3 of the atmosphere without routine in-situ measurements. However, spatial gradient and atmospheric variability is very small in this part of the atmosphere, and thus it is not important in our study.

5. L190: As you mention, nine AirCore profiles is inadequate to evaluate CT2015 stratospheric CO₂. Perhaps you could use the other, (much) older balloon-borne or ER-2-borne stratospheric CO₂ measurements (e.g.,BOS (<https://espoarchive.nasa.gov/archive/browse/bos/Balloon>), STRAT (https://espo.nasa.gov/strat/content/STRAT_Science_Overview), ASHOE, etc.), or the more recent HIPPO and ATom aircraft profiles that often reach above the tropopause altitude, especially in wintertime.

Stratospheric CO₂ has very small spatial gradient (Andrews et al., 2001) that contribute to total spatial gradient of total column CO₂. Thus it is not important for our study. We only need reasonable stratospheric CO₂ results to compensate the missing column information of stratospheric CO₂. We could've simply expand the partial column results to the total column since we know we have ~ 70% of the column with most of the spatial gradient signals; however, we opt to use the CT modelled stratosphere CO₂ to account for the effect of slightly delayed seasonal cycles in stratosphere.

6. L201: It's not clear to me why you compute the high CT bias by using the partial column comparisons. Why don't you integrate the entire CT and AirCore profiles and compare those values?

The top 1/3 partial column is the part from CT that we use to calculate total column CO₂, in addition to aircraft and tower measurements. Integrating entire vertical profiles of AirCore will introduce extra uncertainty of AirCore measurements near surface, which is mostly related to the seal time of the AirCore that is not relevant to the stratospheric part of the measurements. We have modified the sealing process for recent AirCore samples.

7. L206: This is unclear: if the stratosphere doesn't matter for your analyses, why include it at all?

Please also see answers for question 3 and 5. We want the results for total column in addition to the partial column that ceiled at 8 km, to provide baseline spatial patterns for comparison with total column retrievals from remote sensing instruments. For the stratosphere, we show in our study that Carbon Tracker's performance is good when compared with individual AirCore profile. For long-term averages, Carbon Tracker results are good enough for our study.

8. Fig 3 caption: What are the black dots?

Black dots in Fig.3 shows the aircraft data above 2km. It is showed in the figure legend.

9. L250: I don't understand why this sentence does not end after "It demonstrates that there is a lot of important information in the vertical profile."

We state "It demonstrates that there is lot of important information in the vertical profile that is diminished in observations of the total column". We think it is important conclusion in our study: most spatial gradient signals reside in lower troposphere (that's why it is important for measurements to be sensitive to this part of atmosphere). This conclusion cannot be demonstrated by column measurements.

10. Fig. 7: It seems strange that you would not include de-trended averaged TCCON XCO₂ for comparison in regions that have long-term TCCON measurements (i.e., MW and SM). Additionally, Figure S1 would be an ideal place to show the SGP TCCON total column measurements.

Please see response to general comment.

11. L338: What does "deepest drawdown" mean? The lowest minimum value? The largest amplitude?

We mean the largest amplitude in seasonal cycles among the 8 regions. We will clarify this in the revised paper.

12. L337-339: "It is interesting that the deepest drawdown is seen in region NM, not in region MW that encompasses the very intensive agricultural activities in the U.S. midwest, which suggest the possibility of strong upwind influence in the NM region." I agree this is interesting. Could the authors say something more about possible causes of this effect?

This is evidence that column CO₂ is not dominated by surface flux. Even though the boreal uptake is the largest in MW in summer due to intense plant activities, the column CO₂ does not show the lowest value in MW because transported signals have major contribution on column CO₂.

13. L343: Again, what does “strength of summer drawdown” mean here?

“strength of summer drawdown” means the variation amplitude in seasonal cycles. We will clarify this in the revised paper.

14. L373: This sentence is misleading, regarding Keppel-Aleks et al., 2012: “Thus they also propose that the variations in column CO₂ are mainly driven by large-scale flux and transport.” In Keppel-Aleks et al., 2012, they also state (in the abstract): “Rather than obscure the signature of surface fluxes on atmospheric CO₂, these synopticscale variations provide useful information that can be used to reveal the meridional flux distribution.”

Keppel-Aleks et al.(2012) finds similar results as our study, and states in their abstract that “New observations of the vertically integrated CO₂ mixing ratio <CO₂> from ground-based remote sensing show that variations in <CO₂> are primarily determined by large-scale flux patterns.” They specifically state in sector 3.1 that “In summary, the comparison between drawdown in <CO₂> and eddy covariance flux confirms that while regional information is contained in column observations, **these regional flux signals are obscured by larger-scale variations in <CO₂>** even on the short timescale.” We both agree with this. Since column CO₂ primary reflects large-scale flux, it is logical that local signals are significantly “diluted” in the total column.

The later statement is actually referring to their method to use both potential temperature and column CO₂ to estimate flux gradients (the distribution), but not the flux itself. This method is useful to evaluate biosphere models.

15. L373: That large-scale circulation drives almost half (~40%) of the N-S gradient in XCO₂ was also shown in Wunch et al. (2013) through the interannual variability of the seasonal cycle amplitudes.

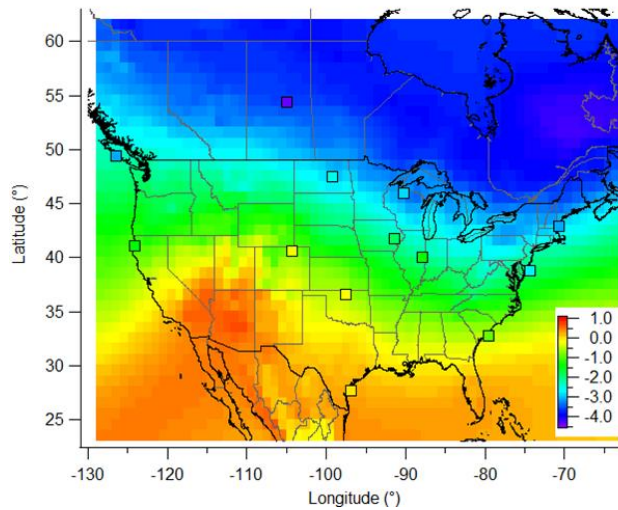
We will cite Wunch et al. (2013) in revised paper. However, we should also acknowledge that interannual variability is not the same statistic metric as the long-term averaged spatial patterns we discuss in our study. We should expect that smaller scale features (local/regional fluxes) are further dampened in long-term time scale.

16. Fig 9: Why do the aircraft measurements appear to disagree significantly with CT in panel (c) in the SGP/Colorado region, and the site just south of lake Michigan?

CT in panel (c) shows the partial column CO₂ between 800 hpa to 330 hpa. For SGP and CAR (-0.30 and -0.23 ppm, respectively, based on aircraft measurements), CT results show -0.74 and -0.57 ppm (these numbers are provided in the SI in the revised paper). The mismatches are within ~0.4 ppm which is similar to our uncertainty levels. There are a few possible reasons for these mismatches. The aircraft is designed to sample 0.1° × 0.1° area, while CT is 1° × 1° spatial resolution. Thus CT may show smoother results. In this case, CT compared better with aircraft measurements in background sites than those influenced by local anthropogenic emissions significantly. SGP is highly polluted by Oil and Gas operation. CAR is also influenced by ONG operations; however, the mountain terrain is challenge for the model too.

For the site HIL (south of Lake Michigan), we have recently found unrealistic high CO₂ levels from some profiles that might associated with cabin air contamination. As a precaution, we have removed this part of data (including both 2012 and 2013 summer) in our study after comparing mid-troposphere measurements with the other 4 aircraft sites (LEF, WBI, CAR, and DND) around. We have updated relevant results (including figures) in the revised paper. This update has minimal influence on the regional averages, since we have abundant data in MW region. This update yields slightly lower column averaged CO₂ in HIL, which better match the CT 2015 (see updated figure below). Another update has been made on aircraft based column CO₂

to fully account for the influence of the temporally uneven sampling frequency. In addition, there are other reasons that model cannot produce perfect results, for example, the transport error may also play a part in the mismatches.



17. L443: I would call 4 ppm a large difference. Please remove “only” from this sentence and quantify the “large spatial gradients” observed below 2 km.

We will remove ‘only’. 4 ppm is smaller compared to the 6 ppm in the SCIAMACHY retrievals in Europe. Spatial gradients below 2 km are discussed in details in section 3.1, and presented in Figure 4, with a maximum difference of ~15.5 ppm between MW and SM in summer on long-term averaged basis.

Technical comments:

We have made changes according to the reviewer suggests.

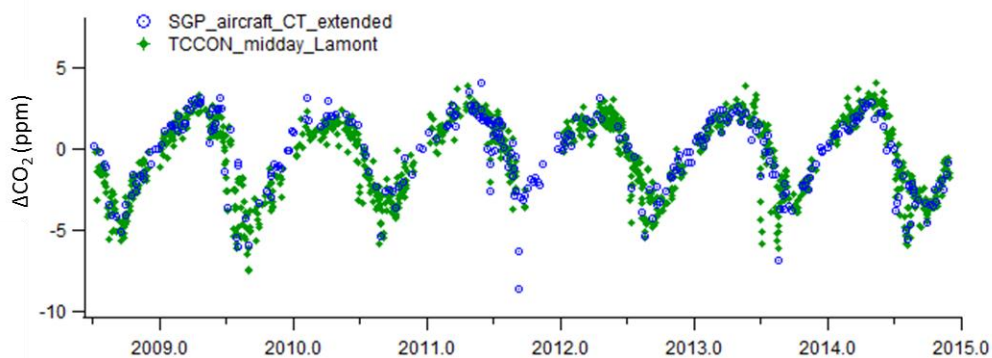
Reply to Reviewer:

Thank you for reviewing our paper.

General comments:

In general, this paper is well-written and is a useful contribution to the literature. I have only a couple serious issues with the paper. First, since this paper is about columns, it would be useful to show direct comparisons of their aircraft-derived XCO₂ to TCCON, to get a sense of differences in remote sensing with respect to a similarly accurate measurement. Second, sometimes they seem to argue that nearly all spatial variability in XCO₂ comes from large-scale + remote fluxes and transport, rather than regional-scale fluxes. Other times (such as in the main body), they argue that a significant contribution comes from large-scale + remote fluxes and transport, but a significant contribution also comes from more regional-scale fluxes (within North America in this study). The latter is more in agreement with their data and specifically their removal experiment of section 3.4, so we suggest they rewrite the paper to stress that both mechanisms affect the horizontal structure of XCO₂.

We agree with the reviewer that it will be interesting to compare TCCON with aircraft + CT based total column CO₂. The following figure can give us some ideas about this comparison. TCCON values in this figure are daily averages computed from mid-day data (10 to 15 LST). Outliers in TCCON data are filtered out, by using 3.S.D threshold of residuals (with iteration) from a quadratic fit on data for each day.



TCCON Data DOI [10.14291/tcon.ggg2014.lamont01.R0/1149159](https://doi.org/10.14291/tcon.ggg2014.lamont01.R0/1149159)

TCCON reference Wunch, D., G. C. Toon, J.-F. L. Blavier, R. A. Washenfelder, J. Notholt, B. J. Connor, D. W. T. Griffith, V. Sherlock, and P. O. Wennberg (2011), The total carbon column

observing network, Philosophical Transactions of the Royal Society - Series A: Mathematical, Physical and Engineering Sciences, 369(1943), 2087-2112, doi:10.1098/rsta.2010.0240. Available from: <http://dx.doi.org/10.1098/rsta.2010.0240>

However, it is not an apple-to-apple comparison between our aircraft-based column CO₂ and TCCON. The sampling time and location are different. Aircraft sampling typically takes ~ 30 min to get the whole profile through downward spiral, mostly within 0.1° of the site location. For TCCON that sampling the whole column instantly at an angle, the sampling time and the actual sampling location (especially at high altitudes), may be far away from our aircraft measurements. Mismatches caused by both should be examined carefully if we want answers for accuracy, which should be the topic of another in-depth study. In addition, we need to acknowledge that the aircraft and tower measurements are calibrated on WMO scale; however, direct calibrations of remote sensing instruments are not available. It makes more sense to compare TCCON against calibrated measurements for accuracy instead of the other way around.

Regarding to reviewer comments on large-scale + remote fluxes and transport:

We do not mean that regional/local fluxes have no influence on long-term averaged column CO₂ spatial pattern. But the major contributor is transport, instead of surface flux. In addition to our observation that long-term column CO₂ spatial gradients pattern is smooth, and mainly reflects large-scale circulation pattern, our results from CT experiments showing that 50% of North-South gradient are due to Eurasia flux, which is stated in both abstract and conclusion parts. Since Eurasia boreal region is obviously not the only upwind location with significant CO₂ sources, (upwind Canadian region is likely contribute to transport signal too), we actually expected **larger than 50%** transport influence in total. We clarify this point in the revised paper.

Though the authors discuss at length their use of CT2015 to extend the aircraft profiles from 330 hPa to the top-of-atmosphere, they don't really discuss the potential errors from the fact that the aircraft measurements don't go all the way to the surface. While some sites do sample very close to the surface (e.g. 0.2 km at SGP), other sites don't even sample as low as 1 km AGL (e.g. CAR: 2.2 km agl, HIL: 1.1 km agl). Because the concentration can change quickly near the surface, the authors need to acknowledge this source of error, and ideally estimate its potential magnitude. They could do this by taking full CT profiles for their sites and comparing the column extended their way (lowest value held constant) vs. the CT value. They can also estimate it based on tower observations for a few sites.

The reviewer has mistaken the unit we use for elevation and altitude. We use 'above sea level (asl)' instead of 'above ground level (agl)' in our study, and the information is presented in S Table 1. CAR is located on a high elevation terrain, as stated in Line 143. There is no < 1km (asl) measurements because the averaged surface elevation is already 1.5 km asl. The lowest layer of aircraft measurements at CAR is ~ 2.1 km asl, which is ~ 0.6 km agl. HIL does sample below 1 km asl; the lowest level is ~ 600 m asl (surface elevation is ~200 m asl). Most regions we discuss in this study also have tower measurements below 1km asl, although aircrafts can sample even lower than the highest inlets of some towers, as we can see from Fig. 5 and Fig. 6. We have a few layers of measurements below 800 hPa for all regions (except MC with 1.5km surface elevation), as we can see from in Fig.5 and Fig.6.

Regarding to the reviewer's comment that "the concentration can change quickly near the surface", is the reviewer referring to nighttime measurements? The aircraft profiles are taken at late morning and early afternoon (data outside 10:00-17:00 local time are excluded in this study), during which time the PBL are generally well-mixed. The tower data we use in our study are also daytime data only, which are stated in our section 2.1. We have observed consistent daytime CO₂ from different heights in tower measurements, even during summer. The following figures are from our tower data:

https://www.esrl.noaa.gov/gmd/ccgg/about/co2_measurements.html

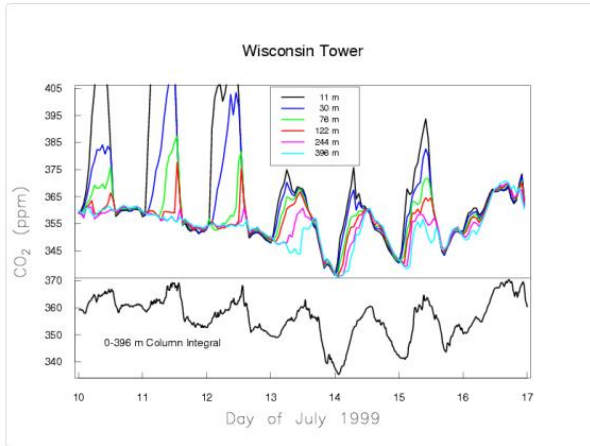


Figure 5a. Measurements of CO₂ by a continuous in-situ analyzer at a tall tower during the summer in northern Wisconsin. The top plot show the CO₂ values at six different heights on the tower.

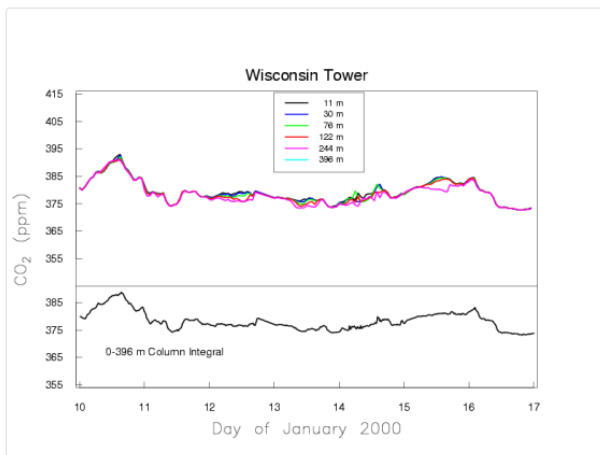


Figure 5b. Measurements of CO₂ by a continuous in-situ analyzer at a tall tower during the winter in northern Wisconsin.

Finally, their section on Reuter et al. (2014, hereafter R14) doesn't fully fit in with the rest of the paper. Specifically, they show that CarbonTracker (CT) agrees well with aircraft over North America. This is not surprising, given the excellent coverage of surface sites in North America, which CT assimilates. However, this does NOT guarantee that CT will be right everywhere, which they seem to imply throughout the paper. They need to stress that this work validates CT in North America specifically. Anywhere else, and they are merely speculating. Also, they focus on the "hot spots" in the R14 map, which are likely due to inhomogenous SCIAMACHY spatiotemporal sampling as much as anything, and may disappear in a regional inversion. Regarding the European sink, the stations that CT assimilates are all in Western Europe, and much of the controversy is really how much sink is portioned between the Europe and Eurasian Boreal Transcom regions, as discussed in both R14 and Reuter et al. (2016). Their central argument that the spatial patterns of XCO₂ from R14 are unphysical is qualitative at best, and, from this author's perspective, partially based on the unfortunate color scheme (rainbow) chosen by R14 which can accentuate very small spatial differences. They should tone down the language to something more like to say that the spatial patterns seem unphysical, but more work would be required to really rebut their physicality. They also need to cite Reuter et al. (2016), which gives a thorough overview of the "European sink controversy".

The reviewer agrees that the column CO₂ spatial pattern from SCIAMACHY retrievals is "unphysical". From our comparison with CarbonTracker, which is proven to be trustworthy for the long-term spatial pattern over the U.S., we think the column CO₂ spatial pattern from SCIAMACHY retrievals is unrealistic and disagree with our understanding of transport. It is important to point out these in our study.

We think it is reasonable to believe that CT produces trustworthy results even outside North America, for the following reasons: (1) CT-Europe that simulate more surface measurements shows similar results as CT. (2) The transport in CT is reasonably well, supported by the good simulation of SF₆, a tracer for large-scale transport (see https://www.esrl.noaa.gov/gmd/ccgg/carbontracker/CT2016_doc.php#tth_sEc6, section 6.2). (3) The reviewer seems to suggest that we cannot judge the model permanence in Europe because we don't have the truth to compare with, unlike the well-calibrated aircraft profiles we have in North America. But that's the case for all CO₂ models over Europe. At least for CT, it

compared well with N.A. aircraft measurements, even though aircraft measurements are not assimilated in CT. This gives us more confidence for the CT model.

Regarding to the spatial patterns of SCIAMACHY in Reuter et al.(2014), it is unlikely the inhomogeneous spatiotemporal sampling is the major reason for spotted feature, since 8 years of data are used to generate this spatial pattern. We do not propose that the conclusion of R14 about the large European carbon sink is wrong. However, it is important to point out the serious issue that this study use unrealistic spatial pattern. Based on our knowledge of transport, a smooth spatial pattern is expected, especially after averaging 8 years of data. We do not agree with the reviewer that the “unfortunate color scheme (rainbow) chosen by R14” is the reason for the unrealistic spatial pattern. We use the same rainbow color scheme and the same 6 ppm maximum color scale as R14 in our Fig. 11, in order to compare with Reuter et al. We do not see the spotted feature on similar spatial resolution; instead we see gradual spatial patterns that match our understanding on transport (Keppel-Aleks et al., 2012 find similar results about the significant influence of large-scale transport).

We will cite Reuter et al. 2016 for European sink. However, the main purpose of our study is not to discuss the European sink. We intend to show a smooth spatial pattern of column CO₂ (based on well-calibrated measurements) that match our understanding of transport, which should be a baseline for current and future remote sensing retrievals.

Specific and technical comments:

L54: Suggest you add language such as “or else regional-scale biases can result” and cite Chevallier et al. (2014).

We cite the Chevallier et al. (2014) in the Line 88.

L65: While satellite retrievals of XCO₂ can certainly have regional biases, the Inoue et al. (2016) paper is hardly thorough. It discusses one particular retrieval (the NIES retrieval) of GOSAT data, and in fact the authors appear to cherry-pick the biases of 2.09 and 3.37 ppm they list, which come from stations with the fewest collocations (3 and 1, respectively). Most of the stations in that paper have biases less than 1ppm, consistent with their comparison to TCCON, and that of Kulawik et al (2016). The authors should give a fairer representation of Inoue et al, including their TCCON comparisons, and mention the mean biases relative to TCCON given in Kulawik et al. (2016).

The reviewer suggests that comparison between GOSAT and TCCON is fairer. The Inoue et al., 2016 compared GOSAT retrievals with aircraft based column CO₂ after correcting GOSAT retrievals against TCCON. This is independent evaluation; however, comparison with TCCON after correction (using TCCON data as reference) is not. We don't think comparing with TCCON is a better approach than comparing with aircraft-based column CO₂. While TCCON shares some similarities with satellite retrievals column CO₂ considering both use remote sensing technique, TCCON itself has known bias. TCCON cannot be directly calibrated, unlike aircraft profiles. Well-calibrated measurements should be a prefer 'truth' to compare with.

We will provide the information that 20 out of 27 stations in Inoue et al. (2016) study shows difference smaller than 1 ppm compared with aircraft-based column CO₂.

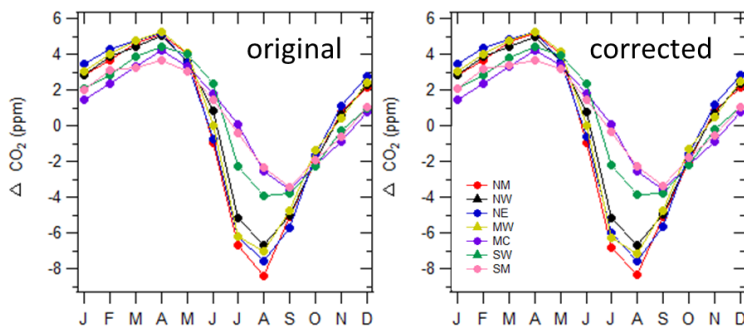
L88: To the 2001 and 2004 papers they cite, they should add Chevallier et al. (2014), which more explicitly demonstrate this.

We cite the Chevallier et al. (2014) in revised paper.

L119-125: Regarding the recently-discovered high humidity bias. To me, this seems like a pretty large error, especially if the mean / typical correction is 0.5 ppm! Since this is the first paper to discuss it, a plot seems warranted – authors should plot the estimated error based on humidity, and justify this 1.7% humidity cut-off value they give. Also, the authors aren't entirely clear on the units of "humidity" here. Presumably they mean volumetric mixing ratio = dry air mole fraction; please be more clear, or use a more typical unit (such as mass mixing ratio or specific humidity).

While a 0.5 ppm correction seems to be large, only ~ 4% of total aircraft measurements or ~ 12% of those below 2 km are impacted. The 1.7 % threshold is preliminary, based on data from

2 tower sites; however, our more recent aircraft measurements with larger amount of data find that this threshold is sufficient for data correction. We are still working to better understand and quantify this bias, and testing dryer design to avoid influence of high humidity. To evaluate the impact of this bias on our study, we have compared the partial column CO₂ results (below 330 hPa) before and after the corrections. Please see figures below:



From this comparison, it is safe to say that this correction does not pose an obvious difference on our results. However, for future studies that are not averaging over long-term record like this study, we need to be prudent on this bias.

The unit for humidity here is ppm in mole fraction, which is the mole of water vapor versus whole air. Dry air should not be assumed when we talk about ratio of mole fractions. We clarify the unit in revised paper.

L158: I think the authors mean Figure 3, not 2.

We change it to “Fig. 3”.

L277 – Here is where the authors should discuss potential errors by extending the lowest measurement to the surface (see discussion above in *General Comments*).

Please see response to general comment.

L308 – Please remind the reader here what “partial column” means. I think surface to 330 hPa, but it’s not entirely clear.

We clarify “partial column” in revised paper.

L318 – Suggest you change the sentence to stress that CT captures these features of XCO₂ *over North America* reasonably well. There is absolutely no guarantee that this will be true elsewhere, as discussed in *General Comments*. You can speculate that it will work in other locations, but you don’t show it, so as written this statement is not justified.

We modify the sentence. Please also see response to general comment.

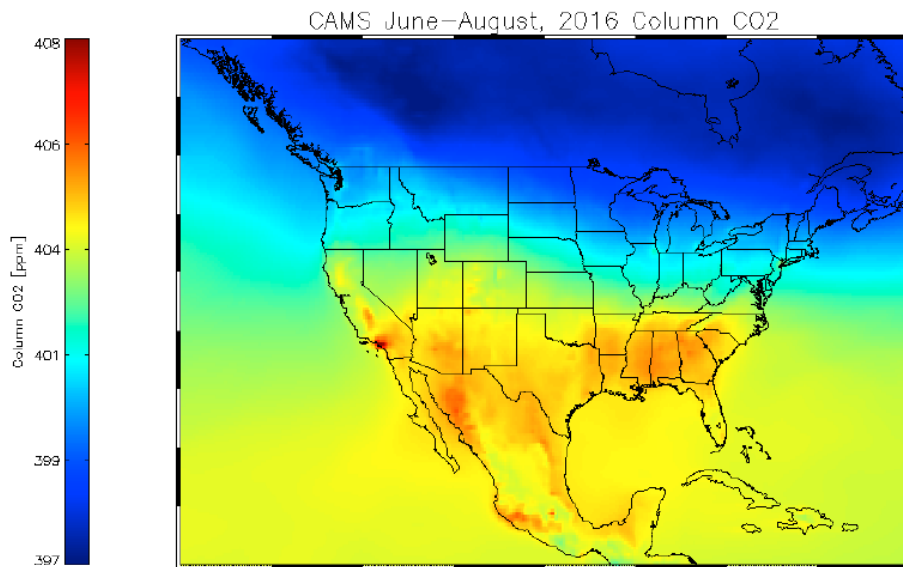
L329 – Please define “drawdown”. Does it mean peak to trough of CO₂ in the seasonal cycle, or the minimum CO₂ relative to MLO? The former is more typically accepted as the definition of drawdown. Then make Fig 8 consistent with your chosen definition.

“Drawdown” refers to the variation amplitudes in the seasonal CO₂ signals that mostly resulted from strong plants activity. We clarify this point several places in the revised paper.

L346 – Again emphasize that the agreement is only shown for North America.

Please see response to general comment.

L348-350 Regarding CT not showing hotspots. This is not necessarily surprising and could be due to CT's limited resolution. I've attached an unofficial plot of the CAMS nrt XCO₂ over North America, for the June-August 2016 average (see e.g. Massart et al. 2016 for details), which has a resolution of roughly 0.25°, and hotspots over L.A. and Mexico city are clearly visible, consistent with the findings of Kort et al. (2012) and others.



It is reasonable that finer grid can show more pronounced hot spots. However, from the CAMS results for 2016 summer, we cannot see random spotted feature like the 8-year mean SCIAMACHY retrievals shows (which are in a much coarser grid).

It is interesting to see whether the hot-spot in LA and Mexico city also exist in the a priori. How does the long-term averaged spatial pattern look like from CAMS? Is the hot-spot feature still pronounced? The long-term averages are those that both Reuter et al. 2014 and our study focus on.

L374-6 : This implies that local/regional fluxes account for ~50% of the horizontal gradient in this case. Authors should mention this fact, rather than argue that virtually all of the spatial gradients come from large scale transport, which is what they state in the abstract.

Please see response to general comment.

L392: Reuter et al (2014) doesn't only use SCIAMACHY; they use GOSAT as well, and in fact, they use a number of different GOSAT retrievals, not just one, and get consistent results from all of them. Statements in this paper should reflect this.

The unrealistic spatial patterns in Reuter et al. (2014) Fig. 2 are SCIAMACHY retrievals. The main purpose of our study is not to discuss the European sink. We intend to show a smooth spatial pattern of column CO₂ that match our understanding of transport, which should be a baseline for remote sensing retrievals. Since our study is not an inversion study, we cannot prove that the inversion results in Reuter et al. (2014) are wrong. We do not intent to focus on the resulting fluxes. Instead, we focus on pointing out that the spatial pattern is unrealistic. The spatial pattern from GOSAT is actually drastically different from SCIAMACHY. Spatial gradient is the backbone of inversion modeling that resolve surface sources and sinks. Their consistent results from different inversions that use drastically different spatial patterns are not assuring, instead, they raise the question that why different inversions based on drastically different spatial gradients (or the unrealistic gradients in SCIAMACHY) can produce consistent results. It is not clear that whether the data are serving as good enough constraints in inversions or the a priori and transport are dominating the results.

L409: The Feng et al. (2016) study is only applicable to global inversions. R14 uses a regional inversion with only observations in Europe, to make themselves insensitive to an overall regional bias, and only use the gradients in the satellite data to infer the European sink. This is somewhat at odds with the Feng et al. study, which shows that much of the apparent European sink comes from satellite observations outside of Europe.

We do not agree with the reviewer that Feng et al. study only applicable to global inversion. From the prospect of inversion setup, there is no guarantee that regional inversion is better than global inversion since reliable boundary condition is still needed for regional inversion. Global constraints are needed to be satisfied. From the perspective of regional satellite data, using regional data makes the inversion less susceptible to extreme bias, such as land-sea bias; however, there are still potential sources of bias within the European region which may be

caused by spatial differences in clouds and aerosols, surface albedo, etc. Small bias is enough to produce drastically fluxes results. Previous study by Masarie et al. (2011) had evaluated the impact of CO₂ measurement bias on CarbonTracker flux estimates and found that 1 ppm bias at one site, the Park Falls, Wisconsin (LEF site in our study), can cause 68 Tg C/yr bias in flux estimate for Temperate North America (~ 10% of the estimated North American annual terrestrial uptake). Flux estimate errors are also found in Europe and boreal Eurasia to compensate for the errors in North America. The importance of small bias is also shown in RT14 Figure 2c that an overall 0.5 ppm spatial gradient over Europe is enough to produce the extra European carbon sink.

Gradients of Column CO₂ across North America from the NOAA Global Greenhouse Gas Reference Network

Xin Lan^{1, 2}, Pieter Tans¹, Colm Sweeney^{1, 2}, Arlyn Andrews¹, Andrew Jacobson^{1, 2}, Molly Crotwell^{1, 2}, Edward Dlugokencky¹, Jonathan Kofler^{1, 2}, Patricia Lang¹, Kirk Thoning¹, Sonja Wolter^{1, 2}

¹National Oceanic and Atmospheric Administration, Earth System Research Laboratory, Boulder, 80303, Colorado, USA

²University of Colorado, Cooperative Institute for Research in Environmental Sciences, Boulder, 80309, Colorado, USA

Correspondence to: Xin.Lan (xin.lan@noaa.gov)

Abstract. This study analyzes seasonal and spatial patterns of column carbon dioxide (CO₂) over North America calculated from aircraft and tall tower measurements from the NOAA Global Greenhouse Gas Reference Network from 2004 to 2014. Consistent with expectations, gradients between the eight regions studied are larger below 2 km than above 5 km. The 11-year mean CO₂ dry mole fraction (XCO₂) in the column below ~330 hPa (~ 8 km above sea level) from NOAA's CO₂ data assimilation model, CarbonTracker (CT2015), demonstrates good agreement with those calculated from calibrated measurements on aircraft and towers. Total column XCO₂ was attained by combining modeled CO₂ above 330 hPa from CT2015 with the measurements. We find large spatial gradients of total column XCO₂ during June to August, and the north and northeast regions have ~3 ppm stronger summer drawdown (variation amplitude in seasonal cycle) than the south and southwest regions. The long-term averaged spatial gradients of total column XCO₂ across North America show a smooth pattern that mainly reflect large-scale circulation patterns ~~rather than regional surface sources and sinks~~. We have conducted a CarbonTracker experiment to investigate the impact of Eurasian long-range transport. The result suggests that the large summer time Eurasian boreal flux contributes about half of the north-south column XCO₂ gradient across North America. Our results confirm that continental-scale total column XCO₂ gradients simulated by CarbonTracker are realistic and can be used to evaluate the credibility of spatial patterns from satellite retrievals, such as the long term average spatial patterns from satellite retrievals reported for Europe which show larger spatial difference (~ 6 ppm) and scattered hot spots.

1 Introduction

Atmospheric measurements of carbon dioxide (CO₂) from ground and airborne platforms have greatly increased our knowledge of the global carbon cycle. Observations of CO₂, including the NOAA Global Greenhouse Gas Reference Network (GGGRN), initially emphasized ground-based measurements. These observations, started by C.D. Keeling, have monitored the CO₂ trend on both regional and global scales for over 50 years (e.g., Keeling and Rakestraw, 1960; Tans et al., 1989). In addition, the frequency and spatial distribution of airborne measurements have increased rapidly in the last two decades, providing important information about horizontal and vertical

36 variability of atmospheric CO₂ (e.g., Gerbig et al., 2003; Choi et al., 2008; Biraud et al., 2013). Routine aircraft
37 measurements from the NOAA/ESRL GGRN monitor the large-scale distributions of a suite of trace gases,
38 including CO₂, under the influence of continental processes (Sweeney et al., 2015). A very successful approach has
39 been to employ commercial aircraft as a platform for CO₂ measurements, such as Japan's CONTRAIL
40 (Comprehensive Observation Network for TRace gases by AirLiner) project which has provided valuable
41 information for CO₂ in the high troposphere and lower stratosphere (Machida et al., 2002; Machida et al., 2008).
42 Vertical profiles of atmospheric CO₂ reflect the combined influences of surface fluxes and atmospheric mixing.
43 Vertical profiles are particularly useful for evaluating vertical mixing in atmospheric transport models that are used
44 for inverse modeling (e.g. Stephens et al., 2007) to derive estimates of regional- to continental-scale CO₂ sources
45 and sinks (e.g., Tans et al., 1990; Gurney et al., 2002; Gurney et al., 2004; Ciais et al., 2010;).

46 While CO₂ sources and sinks are better constrained at the global scale by global mass balance, it remains
47 challenging to accurately resolve CO₂ sources and sinks at regional-to continental-scale, the apportionment of which
48 depends on relatively minor variations of the observed spatial and temporal patterns of CO₂. When averaging over a
49 few months and longer the largest portion of the variations over continents results from hemispheric-scale terrestrial
50 uptake (photosynthesis)/emissions (respiration) and fossil fuel emissions, while regional net fluxes can make a
51 relatively small contribution to the signal. For example, a simple mass balance argument shows that all U.S. CO₂
52 emissions from fossil fuel burning (~1.4 Pg yr⁻¹) create a total column enhancement of only 0.6 ppm on average in
53 air parcels over the East Coast compared to the West Coast and Gulf Coast if we assume a residence time of the
54 emissions of 5 days to pass the contiguous U.S. (~8×10¹² m²).

55 With careful calibration, air handling, and analysis, the uncertainties of in-situ measurements are less than 0.1
56 ppm. However, in-situ observation networks are sparse in global and regional coverage. Remote sensing data
57 radically increase the number of observations and capture under-sampled regions. It is likely to have a valuable
58 impact on our understanding of the carbon cycle. However, both the precision and the potential of even very small
59 systematic biases in remote sensing measurements need to be carefully evaluated. Vertical profiles from in-situ CO₂
60 measurements have been used to evaluate ground-based total column XCO₂ (X stands for dry mole fraction)
61 determinations, such as those from the Total Carbon Column Observing Network (TCCON) (Washenfelter et al.,
62 2006; Wunch et al., 2010; Messerschmidt et al., 2011; Tanaka et al., 2012). The uncertainty of TCCON total column
63 CO₂ is reported to be 0.4 ppm (1σ) after comparison to aircraft measurements (Wunch et al., 2010). Vertical profiles
64 are also used to evaluate satellite retrievals of total column XCO₂, such as those from the Tropospheric Emission
65 Spectrometer (TES)(Kulawik et al., 2013) and the Greenhouse Gases Observing SATellite (GOSAT) (Inoue et al.,
66 2013, 2016; Saitoh et al., 2016). Satellite retrieval products have known and unknown biases (due to errors in
67 spectroscopy, viewing geometry, spatial differences in clouds and aerosols, surface albedo, etc.) that can result in
68 false horizontal gradients in total column XCO₂ for inverse estimates of sources (Miller et al., 2007; Crisp et al.,
69 2012; Feng et al., 2016). After correction for known biases, the mean GOSAT total column CO₂ (NIES retrievals)
70 biases range between -2.09 to 3.37 ppm (mean = 0.11 ppm, S.D.= 1.11 ppm; 20 out of 27 stations show biases lower
71 than 1 ppm) across different aircraft sites over land, compared with aircraft-based total column XCO₂ (Inoue et
72 al., 2016). By comparing with TCCON, the Orbiting Carbon Observatory-2 (OCO-2) retrieval of total column XCO₂

73 was estimated to have a mean difference less than 0.5 ppm with RMS differences typically below 1.5 ppm after bias
74 correction (Wunch et al., 2016). The overall uncertainty of satellite retrievals is relatively large compared with the
75 total column XCO₂ calculated from in-situ measurements. Total column XCO₂ calculated from vertical profiles from
76 the Japanese CONTRAIL project (Machida et al., 2008) and from the NOAA Carbon Cycle and Greenhouse Gas
77 aircraft program (Sweeney et al., 2015) complemented with simulated profiles from a chemistry–transport model
78 above the maximum altitude of the data have uncertainty less than 1 ppm (Miyamoto et al., 2013). The relatively
79 small uncertainty of the in situ-based total column XCO₂ suggests that they can be used to evaluate satellite
80 retrievals of column averaged CO₂. Since aircraft profiles co-located with satellite retrievals are rare, it is useful to
81 consider the statistics of total column XCO₂ fields derived from repeated aircraft profiles over particular locations.

82 The effect of satellite column averaging kernels and a priori profiles when comparing aircraft-based column
83 XCO₂ with GOSAT retrievals has been assessed by Inoue et al. (2013). For the case considered, application of the
84 averaging kernel and a priori profile to simulate total column XCO₂ was generally within ± 0.1 ppm of the density
85 weighted total column, suggesting that the averaging kernels can only account for small part of the overall
86 uncertainty of the GOSAT total column XCO₂ (Inoue et al., 2013).

87 Transparent and objective estimates of CO₂ sources and sinks derived from atmospheric measurements are
88 paramount for validating emissions reduction efforts and other mitigation policies, and for lowering the uncertainties
89 of carbon cycle-climate feedbacks. The latter are major ambiguities in predicting future climate, such as potential
90 uncontrolled CH₄ and CO₂ emissions from warming permafrost in Arctic regions. Satellite retrievals of total column
91 XCO₂ can significantly improve estimates of sources and sinks only if they are sufficiently precise and accurate
92 (~~Rayner and O'Brien, 2004~~; Houweling et al., 2004; [Chevallier et al., 2014](#)), meaning that even very small
93 systematic errors (biases) must be eliminated. Here, we analyze the spatial and temporal variability of column CO₂
94 over North America using well-calibrated CO₂ measurements from aircraft and tall tower, and we use model results
95 from NOAA's CarbonTracker, version CT2015 (Peters et al. 2007, with updates documented at
96 <http://carbontracker.noaa.gov>) to investigate the primary drivers of variability in total column XCO₂. The aircraft
97 data enable direct analysis of column CO₂ characteristics, which is the fundamental step for accurate apportionment
98 of sources and sinks. This study focuses on the long-term averaged column CO₂ gradient and the contributions of
99 different vertical layers to the total column variability. It can serve as a reference for evaluating current and future
100 column CO₂ retrievals from both ground and satellite platforms.

101 **2 Methods**

102 **2.1 Aircraft and tall tower sampling**

103 Aircraft sampling in the NOAA GGGRN intends to provide vertical profiles of long-lived trace gases to capture
104 their seasonal and interannual variability. The aircraft sampling system consists of 12 borosilicate glass flasks in
105 each programmable flask package (PFP), a stainless-steel gas manifold system, and a data logging and control.
106 These flasks (0.7 L each) are pressurized to obtain 2.2 L of sample air from each target altitude. Air samples are then
107 shipped back to NOAA/ESRL for carefully calibrated and quality-controlled measurements. Carbon dioxide is

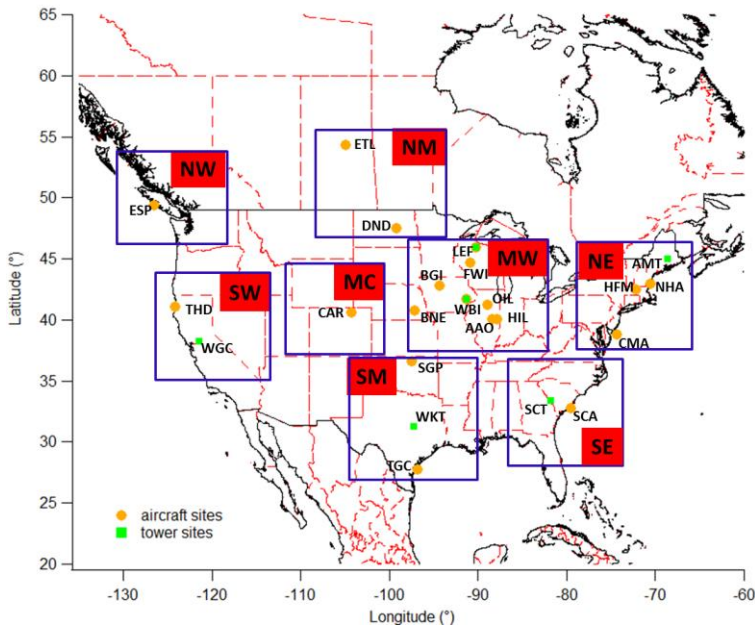
108 measured using a nondispersive infrared analyzer. Long-term measurements at ~15 sites are carried out using light
109 aircraft that can reach 8.5 km. Air samples are collected mostly during late morning to early afternoon, when the air
110 mass within the planetary boundary layer (PBL) is generally well mixed, and CO₂ enhancement near the ground
111 from plant respiration during the night has been mixed throughout the boundary layer. Normally, the aircraft follows
112 a pre-decided route such that most samples are collected within 0.1° of the site location. The sampling frequency
113 varies from site to site, currently from twice a month to once every 1.5 months. For more sampling details, quality
114 control discussions, and an evaluation of the sampling frequency, please refer to Sweeney et al. (2015). More
115 information on the aircraft sites can be found at <http://www.esrl.noaa.gov/gmd/ccgg/aircraft/>. We estimate the
116 uncertainty of individual measurements of CO₂ in flask air (68% confidence level) at 0.08 ppm. However, we have
117 seen evidence of positive biases for samples collected using older flasks that may contain contaminants. Andrews
118 et al. (2014) reported biases that increased from <0.1 ppm in 2008 to an average offset in 2013 of 0.36 ppm. The
119 aircraft sampling protocol was modified starting in August 2014 to mitigate this bias. For samples collected prior the
120 protocol change, laboratory tests showed that new/clean flasks have zero bias, but some older/dirty flasks could have
121 biases of > 1 ppm. This bias is not consistent among individual flasks and increasing over time (Andrews et al.,
122 2014), the potential bias is hard to quantify for measurements before August 2014. Thus, the high bias is not
123 corrected in our study. More recently, low bias has been found in PFP measurements when the ambient humidity is
124 high, based on comparisons of PFP measurements with data from in-situ analyzers at tall towers. We are working to
125 understand and quantify this bias, and for this study we have derived a preliminary correction factor, which shows a
126 linear trend with -1.4 ppm CO₂ offset per 1% above 1.7% of ambient water content (in mole fractions versus whole
127 air). Only ~ 4% of total aircraft measurements or ~ 12% of those below 2 km are impacted by humidity higher than
128 1.7%, for which we have applied corrections before data analysis. The mean correction applied is 0.53 ± 0.4 (1 σ)
129 ppm for the impacted data.

130 The NOAA tall tower network measures CO₂ and other trace gases within the continental boundary layer.
131 Continuous in-situ measurements are conducted using nondispersive infrared (NDIR) absorption sensors and cavity
132 ring-down analyzers. The long-term stability of these systems is typically better than 0.1 ppm for CO₂ (Andrews et
133 al., 2014). Most tall tower sites have more than one air intake height. In this study, continuous in-situ measurements
134 from the highest intake are used to minimize potential influences from local sources. More information concerning
135 the tower sites can be found at <http://www.esrl.noaa.gov/gmd/ccgg/insitu/>. For the column XCO₂ calculation, tower
136 data only from 10:00-17:00 local standard time (LST) on flight days are averaged to one data point per day, as a
137 complement to vertical profiles within the PBL.

138 2.2 Site description

139 We analyze data from 19 aircraft sites and 6 tall tower sites during 2004 to 2014 (see Table S1 for a summary of site
140 conditions). After considering the geographic distribution of these sites in North America, we group them into eight
141 regions for spatial comparisons (Fig. 1). The northern west (NW) and southern west (SW) regions represent the
142 inflow area in the west coast of US, directly downwind of the Pacific Ocean at both higher elevations. The northern
143 mid-continent (NM) region represents the boreal forest and agriculture region in north-central North America. The

144 mid-continent (MC) region represents a dry landscape due to its high elevation (above 1.5 km on average) and semi-
 145 arid climate. The mid-west (MW) region is strongly influenced by agriculture and temperate forest. The southern
 146 mid-continent (SM) represents the south-central humid temperate region, with inflow from the Gulf of Mexico
 147 during summer. The northeast (NE) region represents the temperate forest in north-east coast of U.S., which is
 148 mostly downwind of regions to the west above the PBL, and downwind of its south-west regions within the PBL.
 149 The southeast (SE) region represents the warm temperate region in the south-east coast of U.S.
 150

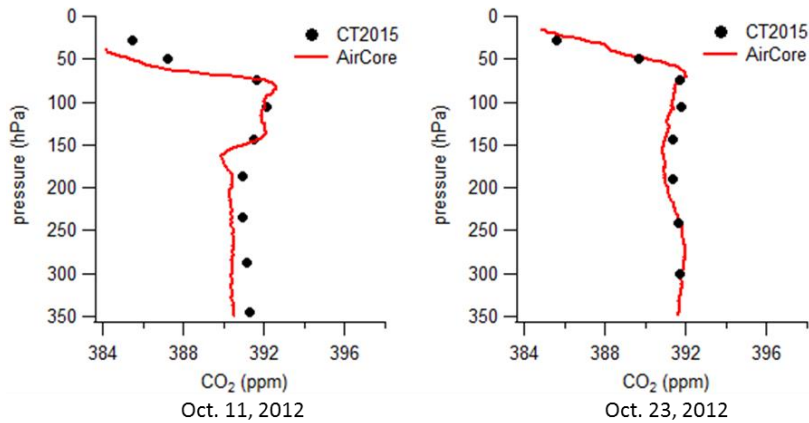


151
 152 **Fig. 1.** Aircraft, tall tower, and high elevation/tower sites in the NOAA GGRN. The eight boxes define regions
 153 that are further discussed for spatial pattern comparison.

154 **2.3 Smoothing of the reference data and column XCO₂ calculation**

155 | We use Mauna Loa Observatory (MLO) as a reference site. The long-term trend of CO₂ measurements from this
 156 | site is removed before combining multiple years of data to calculate long-term averages. MLO is located at
 157 | 19.536°N, 155.576°W, and 3397 m above sea level. Carbon dioxide measurements from this site are widely used to
 158 | represent background CO₂ in the Northern Hemisphere. For our study, a function consisting of a quadratic
 159 | polynomial and four harmonics is fitted to the MLO data, adopted from the method described by Thoning et al.
 160 | (1989). Residuals of the data from this function are smoothed by a low-pass filter with full-width at half-maximum
 161 | in the time domain of 1.1 years. The smoothed residuals are then added back to the polynomial part of the function
 162 | to produce the long-term deseasonalized trend. This trend (see Fig. 23) is subtracted from all aircraft and tall tower
 163 | measurements, as well as from CarbonTracker model results (CarbonTracker - MLO deseasonalized trend,

164 CarbonTracker results presented in this study are the differences relative to observed MLO deseasonalized trend).
165 We use ‘ Δ ’ to represent detrended data in the following text and figures. The choice of reference site is not
166 important for this study, since we focus on examining the relative seasonal patterns of the detrended spatial and
167 vertical distributions of CO₂ instead of the total changes in CO₂ abundance attributed to global surface fluxes.
168



169
170 **Fig. 2.** Carbon Tracker (CT2015) simulations compared with AirCore in-situ measurements in upper atmosphere.
171 AirCore profiles in the left and right panels are sampled near CAR and SGP, respectively.
172

173 We calculate partial column average CO₂ dry mole fraction using tall tower and aircraft data, and the total
174 column by adding simulations of high altitude CO₂ (above 330 hPa, ~ 8 km above sea level) from CarbonTracker.
175 Since geometric height from the onboard Global Positioning System (GPS) (after 2006) or inferred from the aircraft
176 altimeter or pressure altitude is archived with each aircraft measurement, we first convert geometric height (in
177 meter) to pressure (in hPa) for the pressure-weighted column XCO₂ calculation. This conversion uses geopotential
178 data from NOAA/NCEP North American Regional Reanalysis (NARR) (Mesinger et. al, 2004), available at
179 <https://www.esrl.noaa.gov/psd/data/gridded/data.narr.html>, in which the geopotential is a function of latitude,
180 longitude, pressure altitude and time. We interpolate the geopotential field vertically to retrieve pressure, and then
181 calculate dry pressure by incorporating specific humidity data from NARR. Eventually we use a trapezoidal method
182 to integrate over detrended vertical profiles for dry-pressure-weighted column average. For the long-term averaged
183 column Δ XCO₂ calculation, a long-term mean vertical profile is first constructed for each month by combining 11-
184 year detrended data together and then average data in each 40 hPa vertical bin. To look at the long-term averaged
185 total column Δ XCO₂ from individual aircraft sites, we combine aircraft data with upper-layer CT2015 simulations.

186 The NOAA CarbonTracker model assimilates CO₂ measurements from surface sampling networks and tall
187 towers to generate global 3D fields of atmospheric CO₂ mole fraction. The Carbon Tracker model has evolved
188 significantly since Peters et al. (2007). A detailed description of this model is provided in documents available at
189 <http://carbontracker.noaa.gov>. Our study utilizes CarbonTracker results from the 2015 release (CT2015), publicly

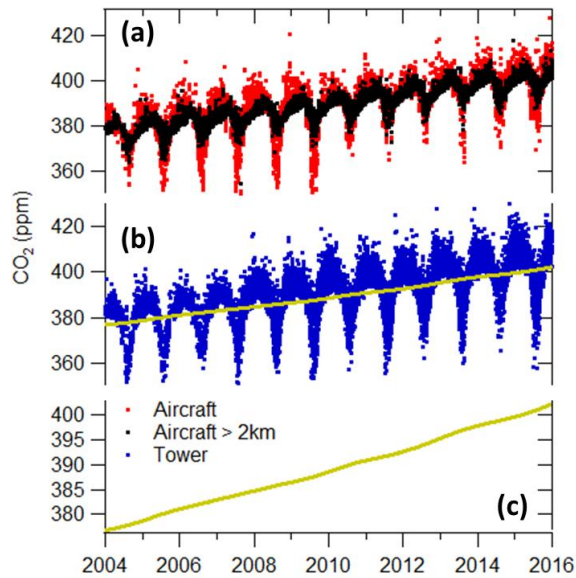
190 accessible at <ftp://aftp.cmdl.noaa.gov/products/carbontracker/co2/CT2015/molefractions/>. This version provides
191 CO₂ mole fraction over North America with 1° × 1° spatial and 3 hour temporal resolutions, which are analyzed in
192 Sect. 3.2 and 3.3. Total column CO₂ calculated from CT2015 global data with 3° × 2° spatial resolution is also
193 presented in the supporting information (SI). We have evaluated the performance of CarbonTracker in upper
194 atmosphere (330 to 0 hPa) by comparing its simulations with in-situ measurements from 9 AirCore profiles (Karion
195 et al., 2010) sampled in 2012-2014. AirCore is a ~150 m stainless steel tube that utilizes changes in ambient
196 pressure for passive sampling of the vertical profile. It is released using balloons and it collects a continuous sample
197 as it descends. It is then measured by an analyzer after it is recovered. More information about AirCore system can
198 also be found at <https://www.esrl.noaa.gov/gmd/ccgg/aircore/>. [All 9 AirCore profiles are taken near SGP and CAR](#)
199 [sites](#). Figure 2 shows examples of AirCore profiles compared with CT2015 in the upper atmosphere, which
200 demonstrates good agreement. We also compare partial column (330 to 0 hPa) averages from the 9 AirCore profiles
201 and CT2015. Results from CT2015 agree generally well with AirCore, with difference ranging from 0.03 to 1.22
202 ppm (mean value equals 0.66 ppm), which suggests that CT2015 may have a high bias that can contribute to
203 0.66×1/3=0.22 ppm overestimate on average to the total column average. However, AirCore is in the process of
204 rigorous evaluation, the differences between AirCore and CT2015 are not well characterized yet since we only have
205 a limited amount of AirCore data. It is unclear whether the potential bias of CT2015 in this partial column is
206 dependent on time or sampling location. Adding a constant bias correction to all regions will not change the spatial
207 gradients that we focus on in this study. Thus no correction is applied when using CT2015 simulations to represent
208 the upper 1/3 of the total column.
209 For uncertainty estimates, we use a ‘bootstrap’ method that uses random resampling and repetition of individual
210 vertical profiles (low bias due to high humidity was corrected), with 100 Monte Carlo runs for each column average
211 calculation. Uncertainty is then defined as one standard deviation of the 100 Monte Carlo results.

212 **3 Results and Discussions**

213 **3.1 Seasonal patterns and spatial gradients**

214 Typically one aircraft profile contains measurements at 12 different altitudes. Column ΔXCO₂ can be computed for
215 each profile using the method described in Sect. 2.3 (Fig. S1). Figure 3 shows aircraft (at all altitudes) and tower
216 data (daily averages for 10:00-17:00 LST data) from all sites used in this study. Aircraft data above 2 km exhibit
217 much smaller seasonal variations than the full dataset, because the variations are mainly driven by CO₂ sources and
218 sinks near Earth’s surface. CO₂ concentration is enhanced in the shallow wintertime PBL primarily due to reduced
219 plant photosynthesis and ecosystem respiration combined with slightly increased fossil fuel emissions. During
220 summer the PBL is deeper, and depletions within the PBL are due to strong terrestrial uptake that dominates over
221 emissions especially during June through August. During summer of 2010 to 2012, CO₂ from aircraft measurements
222 appears higher than other years in Fig.3; however, similar characteristics are not present in tower data. This
223 difference is due to a decrease in sampling frequency at several aircraft sites that resulted in an aliased picture of the

224 | full summer drawdown signals. Since we focus on climatological mean of 11 years of data in our study, this
225 | influence is eliminated by combining 11 years of data together into one “average year”.



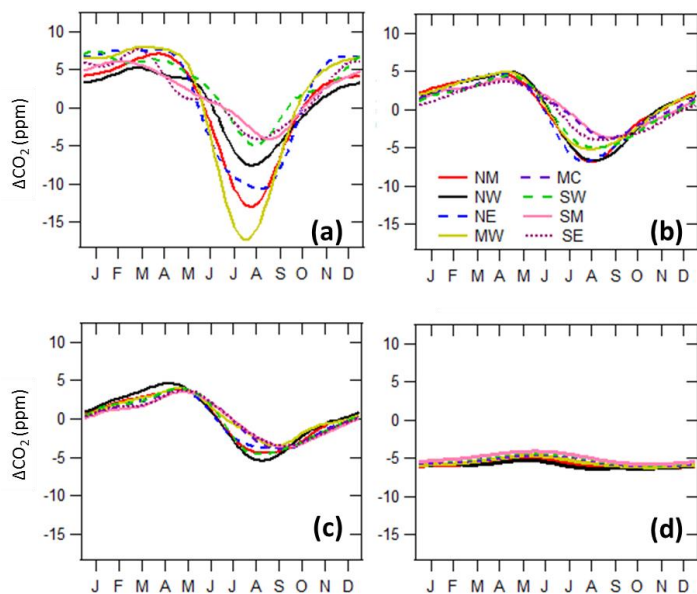
226 |
227 | **Fig. 3.** CO₂ observations from aircraft (a) and towers (b). The yellow line in (b) illustrates the deseasonalized trend
228 | at Mauna Loa (MLO), same as in (c), in which y-axis expanded.

229 |
230 | To investigate the contributions of different altitudes to spatial gradients between regions, we divided all
231 | measurement data into three layers according to their sampling altitudes: below 2 km, 2 - 5km, and 5 - 8.5 km masl
232 | (Fig. 4). Smooth seasonal curves are attained from fitting data with four harmonics using the method described by
233 | Thoning et al. (1989). The peak-to-valley amplitudes of the seasonal cycles below 2 km are the largest among the
234 | three layers for most regions, with a minimum of 10.3 ppm in SM and a maximum of 25.0 ppm in MW. The
235 | seasonal variation amplitudes decrease to 7.7-11.5 ppm in the 2 - 5 km layer, and further decrease to 7.2-10.0 ppm in
236 | the 5 - 8.5 km layer. We also observe that the seasonal cycle drawdown occurs later in the layers above 2 km (see
237 | Fig. S2, which provides similar information as Fig. 4, but seasonal curves from different vertical layers are grouped
238 | by regions to facilitate comparisons of the phases of seasonal cycles). The seasonal CO₂ drawdown below 2 km is
239 | mainly influenced by terrestrial photosynthesis and gradients are influenced by local to regional fluxes, with an
240 | earlier onset of drawdown in southern regions than in northern regions. The seasonal cycle aloft is damped and
241 | lagged compared to the PBL, with influences from throughout the Northern Hemisphere and with spatial gradients
242 | likely driven by large-scale transport. The NW, SW, SM, and SE inflow regions have significant delays of more
243 | than one month in the 2 - 5 km layer compared with the surface layer, which is likely due to the delayed phase of the

244 seasonal cycle in well-mixed air coming from the oceans. Vertical homogeneity of air over ocean was observed
245 during the HIAPER Pole-to-Pole Observations (HIPPO) aircraft campaign (Wofsy et al., 2011; Frankenberg et al.,
246 2016). As air masses are transported further inland, we observe reduced discrepancies of the timing of CO₂
247 drawdown between surface and upper layer air (2-5 km), which may be associated with the increased influence of
248 the land surface in the mid-troposphere due to strong convection over land. CO₂ drawdown in the 5 - 8.5 km layers
249 also occurs later than in the 2 - 5 km layers in most regions; however, differences between these two layers are
250 small. The declining amplitude and delayed phase of the seasonal cycle with altitude have been noted often (e.g.,
251 Tanaka et al., 1983; Ramonet et al., 2002; Gerbig et al., 2003, Sweeney et al. 2015). It demonstrates that there is lot
252 of important information in the vertical profile that is diminished in observations of the total column.

253 We find that the largest horizontal spatial gradients between regions occur below 2 km during summer time
254 (Fig. 4), with a maximum difference of ~15.5 ppm between MW and SM. SM and SW exhibit less pronounced
255 seasonal cycles, which is likely associated with air masses from the Gulf of Mexico and the Pacific Ocean,
256 respectively, whereas MW exhibits a deep summer drawdown (amplitude in seasonal cycles) partially as a result of
257 strong regional forest and crop uptake. Crevoisier et al. (2010) estimated the surface flux over North America using
258 vertical CO₂ measurements and average wind vectors, and reported that annually averaged land carbon flux at the
259 western (including SW region) and southern regions (including SM region) were neutral. The SE region also
260 demonstrates a less pronounced seasonal cycle with weaker summer drawdown-higher summertime levels compared
261 with other northern regions, which may be due to the sea-breeze influence in summer within PBL. In wintertime,
262 CO₂ levels in NE and MW are higher than in other regions, which result from regional fossil fuel and terrestrial
263 biogenic emissions combined with transport from the west and south.

264 Higher altitude data (above 2 km) exhibit only small spatial gradients. In the 2 - 5 km layer, the largest gradient
265 is 4 ppm in summer (Fig. 4b). It further decreases to less than 3 ppm in the 5 - 8.5 km layer (Fig. 4c). Figure 4d
266 shows modeled CO₂ mole fractions from CT2015 for the upper troposphere and above (330 hPa to 0 hPa), which are
267 used to fill in above the aircraft profiles for calculation of total column ΔXCO₂. Spatial gradients in this layer are
268 less than 0.5 ppm, suggesting that the top third of the total column has little contribution to the spatial gradients of
269 the total column.



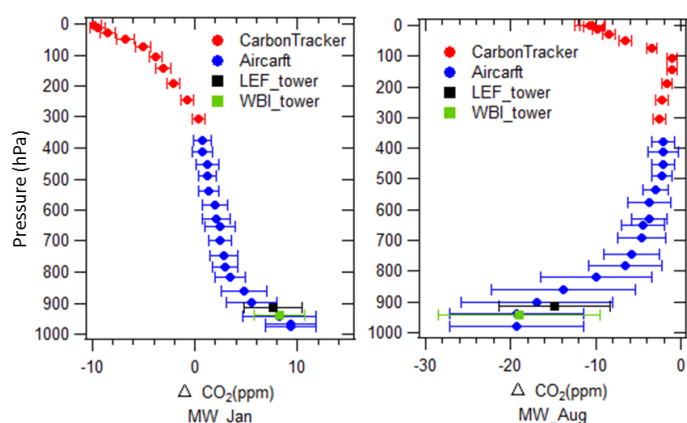
270
 271 **Fig. 4.** Multi-year (2004-2014) average smooth seasonal curves of CO₂ relative to the long-term de-seasonalized
 272 trend at Mauna Loa for different vertical layers: (a). Aircraft and tower data under 2 km, MC is not presented
 273 because only limited data were available due to high surface elevations (>1.5 km on average) in this region; (b).
 274 Aircraft data from 2 - 5 km; (c). Aircraft data from 5 - 8.5 km; (d). CT2015 model results for layers above 330 hPa
 275 (~8.5 km) to 0 hPa (~80 km).

276 3.2 Long-term mean vertical profiles

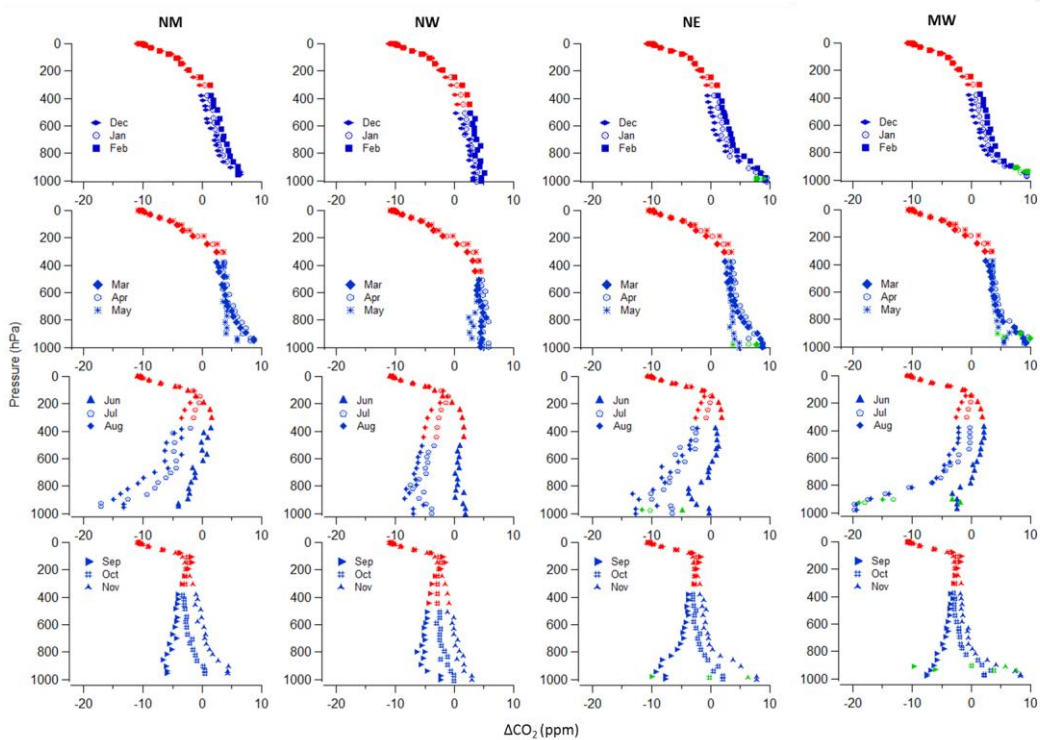
277 To investigate the mean spatial gradients, we first calculate the long-term mean monthly vertical profiles as
 278 described in Sect. 2.3. In addition, each tower serves as one additional layer in the mean profile. The long-term
 279 mean tower data generally fit well in the vertical profiles from measurements of aircraft samples (Fig. 5 and Fig. 6),
 280 suggesting that the biases described in Sect. 2.1 above do not significantly affect the long-term mean. To attain
 281 profiles of the entire atmospheric column, upper layers (330 to 0 hPa) are filled in by CT2015, and the lowest data
 282 point of the measured profile is extended to ground level, defined by the mean surface elevation in that region.

283 Figure 5 presents two examples of long term mean profiles with data variability, which is the one standard
 284 deviation for each 40 hPa bin of aircraft data or for all flight-day tower data. Variability as large as 20 ppm is seen
 285 within the PBL in the MW region in summer, which is due to strong and heterogeneous surface vegetation uptake
 286 and ecosystem respiration combined with day-to-day changes in wind direction. All long-term mean monthly
 287 vertical profiles are presented in Fig. 6, which shows the mean temporal and vertical variability of CO₂ in each
 288 season, and further demonstrates the vertical propagation of seasonal CO₂ due to changes of surface flux. In

289 wintertime, monotonic decrease of CO₂ with altitude can be observed from all regions, in which high PBL CO₂ is
 290 mainly driven by surface emissions and reduced vertical mixing (Denning et al., 1998; Stephens et al., 2007).
 291 Surface CO₂ decreases dramatically in the growing season in those regions influenced by high plant activity, such as
 292 NM and MW regions. For the summer vertical profiles in NE and SE region (east coast of the U.S.), the CO₂ mixing
 293 ratio is elevated in the layer under 900 hPa followed by significant decreases in upper layers until 750 hPa, and then
 294 increases with altitude until tropopause (Fig. 6). This is likely a feature of sea breeze influence. Lower-troposphere
 295 air from the sea, lacking terrestrial uptake of CO₂, typically has higher CO₂ in summer compared with inland air.
 296 Polluted air previously advected offshore can be brought back along with sea breeze. Without significant vertical
 297 mixing over the marine surface, high levels of pollutants remain in those air masses. The convergence of sea breeze
 298 with prevailing wind moving offshore may create a period with a stalled frontal structure that can aggregate air
 299 pollutants (Banta et al., 2005). The convective internal boundary layer structure of the sea breeze system can
 300 significantly reduce mixing height (Miller et al., 2003), and also induces higher CO₂ levels. When the sea breeze is
 301 not dominant, air advected from southwest and west (the land) can also bring in polluted air with high CO₂ since this
 302 region is downwind of continental U.S. emissions (Miller et al., 2012).

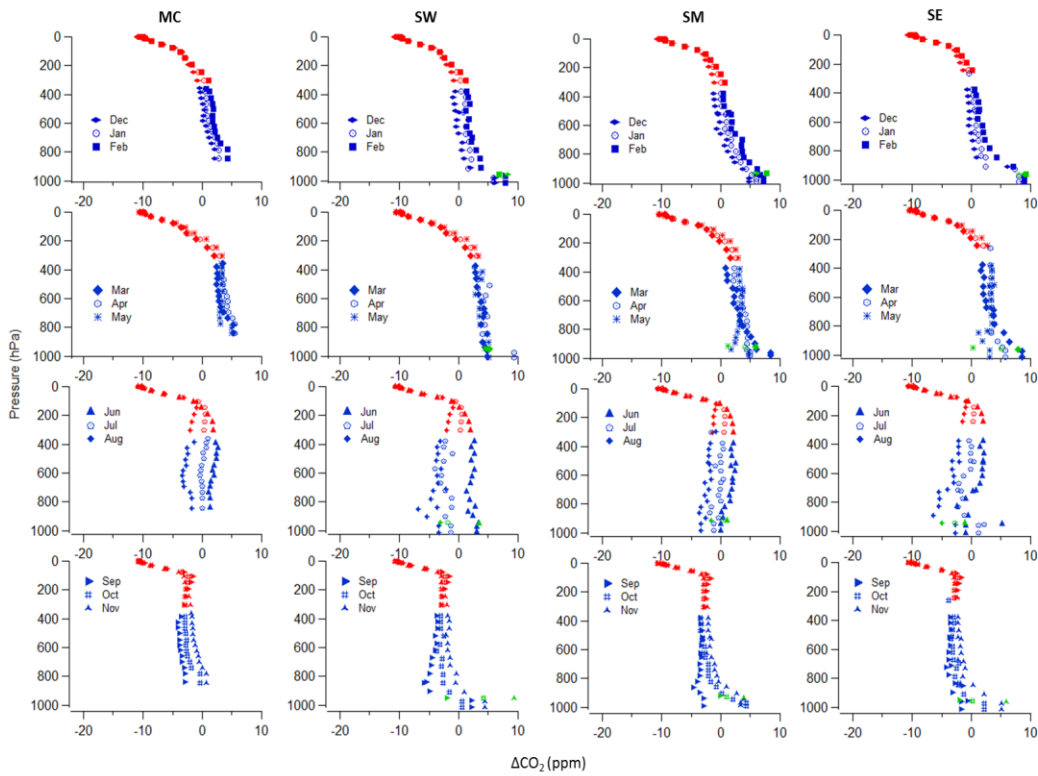


303
 304 **Fig. 5.** Long-term mean (2004-2014) average vertical profiles in January (left panel) and August (right panel) in
 305 region MW. Error bar shows one standard deviation.



306

307 **Fig. 6a.** Long-term mean (2004-2014) monthly vertical profiles in NM, NW, NE, MW (by column, from left to
 308 right). Blue points were calculated from observations, red points were calculated from CT2015, and green points
 309 were calculated from tower data.



310

311 **Fig. 6b.** Long-term mean (2004–2014) monthly vertical profiles in MC, SW, SM, SE (by column, from left to right).

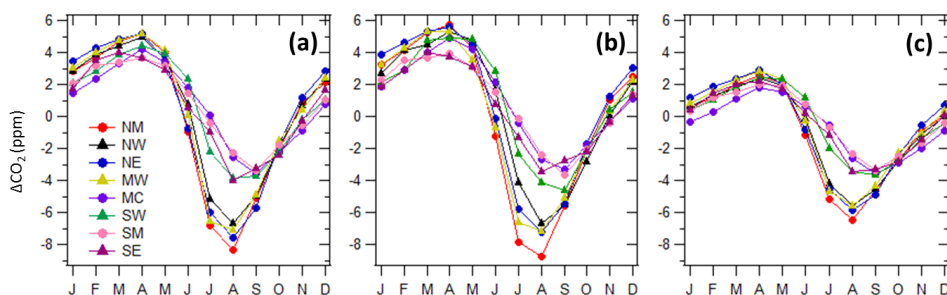
312 Blue points were calculated from observations, red points were calculated from CT2015, and green points were

313 calculated from tower data.

314

315 **3.3 Partial column ΔXCO_2 and total column ΔXCO_2**

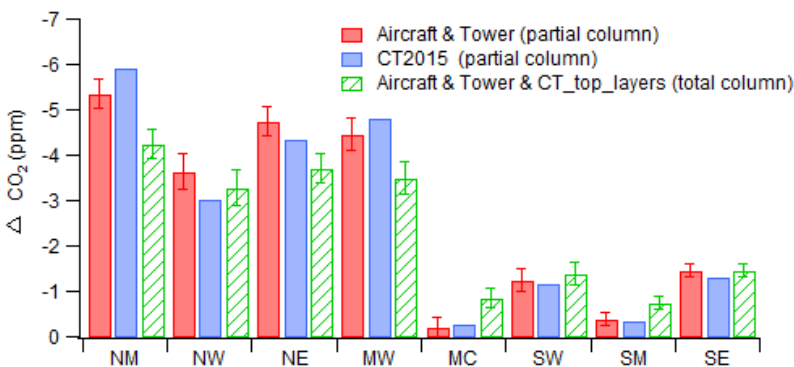
316 Seasonal variations of monthly averaged partial column ΔXCO_2 (below 330 hPa) demonstrate maximum values in
 317 April and minimum values in August or September (Fig. 7a). The largest amplitude appears in NM, with peak-to-
 318 valley difference up to 13.5 ppm. SW, SM, SE, and MC have similar amplitudes of 7-8 ppm, smaller than other
 319 regions. To evaluate the performance of CT2015 on column ΔXCO_2 , CT2015 results are sampled to match the
 320 latitude, longitude, altitude and time of actual measurements. Note that aircraft profiles are not assimilated in
 321 CT2015, so aircraft data are independent of the CT2015 data assimilation. Figure 7b shows monthly partial columns
 322 of ΔXCO_2 calculated from CT2015, which demonstrate good agreement with results from measurements. Only
 323 small seasonal biases exist in CT2015, with high bias occurring mostly in spring and early summer and low bias in
 324 September and October (Fig. S3). The overall differences of monthly partial column ΔXCO_2 (CT2015 -
 325 measurements) mainly fall in the range of -0.64 ppm (5th percentile) to 0.84 ppm (95th percentile) with a mean
 326 difference of 0.13 ppm. These differences are of similar magnitude to the uncertainties of partial column ΔXCO_2
 327 calculated from the measurements (Fig. S4). It is clear that CT2015 captures the long-term mean variations of both
 328 phase and amplitude of partial column XCO_2 reasonably well when compared with well-calibrated measurements
 329 across North America.
 330



331
 332 **Fig. 7.** (a). Partial column ΔXCO_2 calculated from aircraft and tower data; (b). Partial column ΔXCO_2 calculated
 333 from CT2015; (c). Total column ΔXCO_2 calculated from aircraft and tower data and including the top layer data
 334 from CT2015.

335
 336 Total column ΔXCO_2 is presented in Fig. 7c. In regions NW, NM, NE, and MW, seasonal variations of total
 337 column ΔXCO_2 are very similar in both phase and amplitude (8-9 ppm peak to valley). For SW, SM, SE, and MC,
 338 amplitudes are ~5.5 ppm. The smallest spatial gradients occur during May and October, which result in maximum
 339 differences among all regions of only 0.9 and 0.7 ppm, respectively. The largest spatial gradients occur during June,
 340 July and August, which result in maximum differences of 2.4, 4.5, and 4.1 ppm, respectively. It is interesting that the
 341 deepest drawdown (largest amplitude in seasonal cycles) is seen in region NM, not in region MW that encompasses

342 the very intensive agricultural activities in the U.S. mid-west, which suggest the possibility of strong upwind
 343 influence in the NM region. Transported signals have significant influences on total column CO₂.— The summer
 344 ~~drawdown of~~ total column ΔXCO_2 , represented by the June to August average from CT2015, has a magnitude that is
 345 similar to observations with differences no more than 1 ppm (Fig. 8). Based on the seasonal patterns of total column
 346 ΔXCO_2 (Fig. 7c) and ~~strength of summer drawdown~~ the summer column ΔXCO_2 (Fig. 8), we can separate the eight
 347 regions into two groups. The group with NW, NM, NE, and MW, has ~3 ppm stronger drawdown (larger amplitude)
 348 than the group with SW, SM, SE, and MC. For winter total column ΔXCO_2 (December to February average), the
 349 maximum spatial difference is only 1.6 ppm, with the highest total column ΔXCO_2 of 1.2 ppm in NE and the lowest
 350 value of -0.3 ppm in MC.
 351



352
 353 **Fig. 8.** Long-term mean (2004-2014) June to August partial and total column ΔXCO_2 . Error bars represent one
 354 standard deviation from the bootstrap uncertainty calculation (see Sect. 2.3).
 355

356 3.4 Influence of large scale circulation

357 Figure 9 shows long-term mean summer column ΔXCO_2 calculated from CT2015, together with full column
 358 ΔXCO_2 from individual aircraft sites (note that some aircraft sites have less than 11 years of data the CT2015 shows
 359 in Fig. 9, only aircraft sites with more than 6 years of data are presented, the actual values are provided in Table S2).
 360 The fact that total column ΔXCO_2 from CT2015 agrees well with aircraft sites also supports the performance of
 361 CT2015 on a long-term average basis. The observations show a similar summer spatial pattern, with lower column
 362 ΔXCO_2 in the north and northeast regions and higher column ΔXCO_2 in the south and southwest regions (Fig. 9a).
 363 Scattered hot spots of high column ΔXCO_2 associated with surface emissions from megacities, or cold spots
 364 associated with strong local uptake, are not or just barely visible in the long-term average column ΔXCO_2 map at
 365 $1^\circ \times 1^\circ$ resolution. Instead, the wave-like pattern of column ΔXCO_2 over North America reflects large scale
 366 circulation. To support our hypothesis on the influence of large scale circulation, we analyze the long term mean
 367 wind pattern over North America. We can see that air masses from northwest of the continent bring in low average

368 column ΔXCO_2 , while air masses from the south (mainly the subtropical Pacific Ocean and the Gulf of Mexico)
369 bring in high column ΔXCO_2 (Fig. 9b). The zonal gradients over the continent, especially north of 40° N, also
370 reflect long-term average wind patterns; southwest wind corresponds to higher column ΔXCO_2 over the western part
371 of the continent until the wind direction shifts to west-northwest over the eastern part of the continent. This wind
372 pattern matches well with the geographic division of the over/under -3 ppm areas colored in green/blue in the
373 column ΔXCO_2 map (Fig. 9b). Figure 9c and 9d shows partial column averages for free troposphere (800-330 hPa)
374 and lower troposphere (below 800 hPa), respectively. The free troposphere spatial gradient also demonstrates a
375 wave-like pattern. A previous study on the total column CO_2 from ground based Total Carbon Column Observation
376 Network (TCCON) found strong correlation between the mid-latitude column CO_2 and synoptic-scale variation of
377 potential temperature (θ , at 700 hPa), a dynamic tracer for adiabatic air transport (Keppel-Aleks et al., 2012). Thus
378 they also propose that the variations in column CO_2 are mainly driven by large-scale flux and transport. [Analysis on](#)
379 [the interannual variability of the seasonal cycle amplitudes of column \$CO_2\$ in North Hemisphere has also found](#)
380 [significant contribution of large-scale circulations to the north-south gradient \(Wunch et al., 2013\).](#)

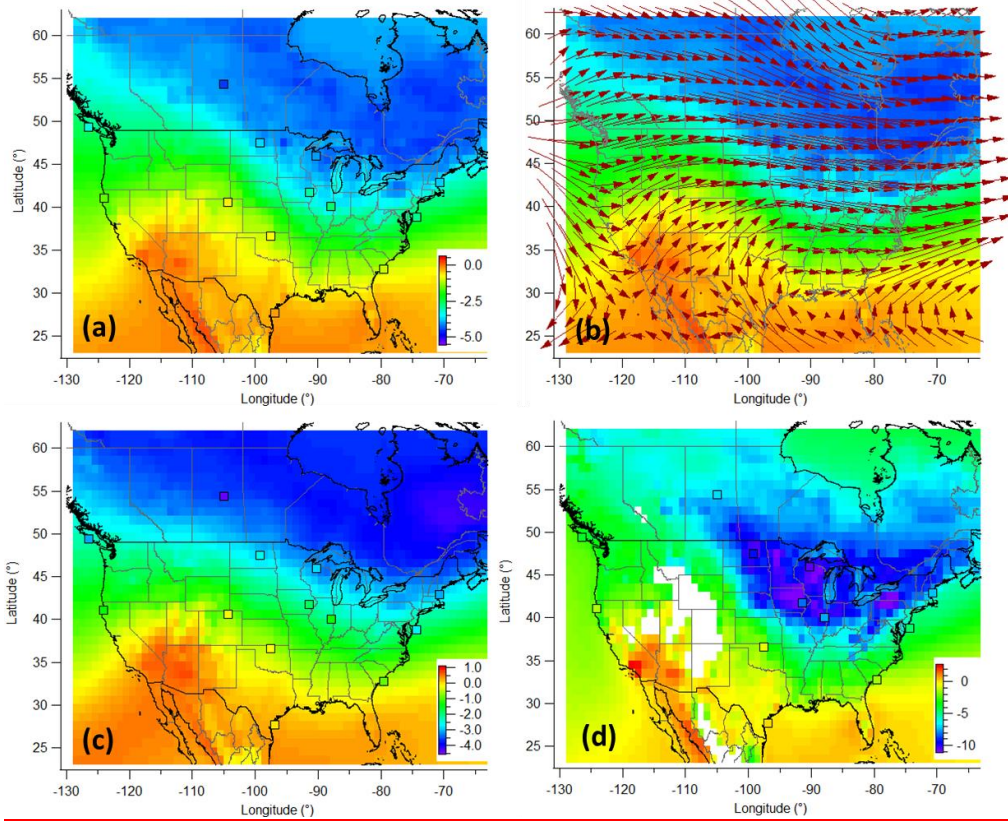
Formatted: Subscript

Formatted: Not Superscript/ Subscript

381 The strong drawdown over northeast North America in summer is a consequence of long-range transport of low
382 CO_2 from northeast Eurasia, in addition to regional terrestrial uptake. Sweeney et al. (2015) notes well-mixed
383 vertical profiles (up to 8 km) of CO_2 , CO, CH_4 , N_2O , and SF_6 from THD, ESP and PFA (Poker Flat, Alaska; 65.07°
384 -147.29°) sites and suggests that air coming across the Pacific was strongly influenced by Asian surface fluxes
385 before being vertically homogenized as it passed over the Pacific Ocean. This well-mixed air forms an important
386 boundary condition in the column CO_2 of air coming into the North American continent. This was best illustrated at
387 sites like PFA where the summertime minimum in CO_2 significantly preceded maximum ecosystem uptake of CO_2 ,
388 implying significant influence of transported air from lower latitude regions from Asia. We further conduct an
389 experiment using Carbon Tracker to investigate the importance of this effect. A control run and a “masked run” are
390 conducted for 2010-2012, in which the Eurasian boreal flux is turned on/off. The MLO CO_2 trend from each model
391 scenario is used as reference background and thus removed before total column ΔXCO_2 calculation. Figure 10 shows
392 the results for 2012 summer, which is an average summer when compared with the 2004-2014 mean pattern (Fig. 9
393 and Fig. 11). The maximum north-south difference reduces to ~2.5 ppm after we turn off the Eurasian boreal flux,
394 compared with ~5 ppm from the control run. [In both control and masked scenarios, the free troposphere partial](#)
395 [\$\Delta XCO_2\$ demonstrates similar spatial patterns as for total column \$\Delta XCO_2\$ \(Fig. S5\).](#) This result combined with results
396 from Sweeney et al. (2015) demonstrates that the transport of low CO_2 resulting from large summertime Eurasian
397 boreal uptake has a large contribution on the overall summer total column CO_2 drawdown in North America.

Formatted: Not Superscript/ Subscript

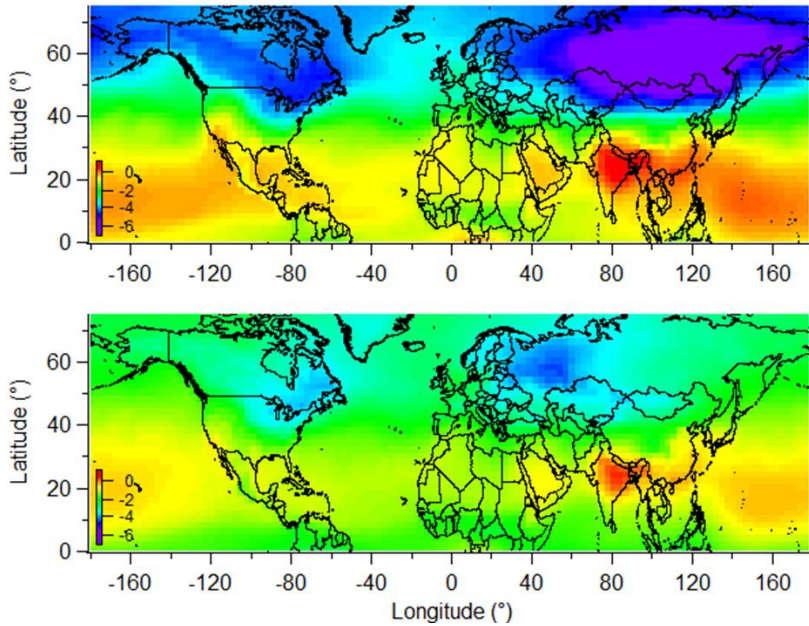
398
399



400

401 **Fig. 9.** Long-term mean (2004-2014) June-August total column ΔXCO_2 from CT2015 in $1^\circ \times 1^\circ$ spatial resolution
 402 with total column ΔXCO_2 for 13 individual aircraft sites in squares (a), and CT2015 column ΔXCO_2 overlaid with
 403 pressure-weighted (1000 hPa to 500 hPa) mean wind vectors for the same period (b). (c) and (d) are similar as (a),
 404 except for free troposphere (800 to 330 hPa) and lower troposphere (below 800 hPa), respectively. Note the different
 405 color scales.

406



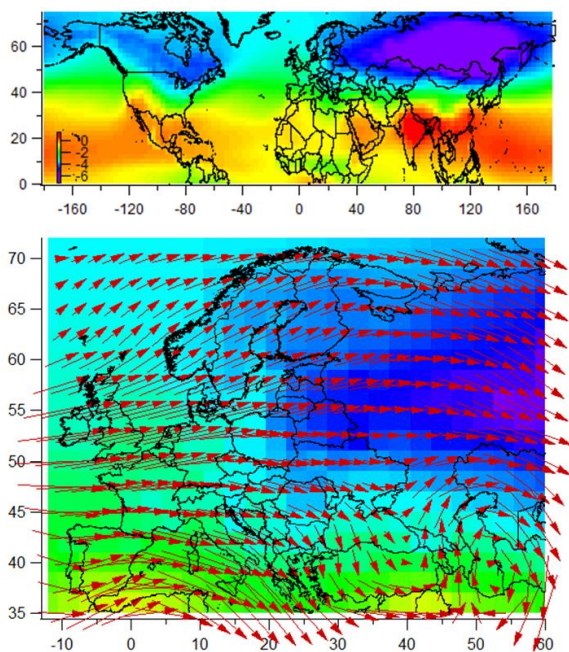
407
 408 **Fig. 10.** Total column ΔXCO_2 from Carbon Tracker control (top panel) and masked (bottom panel, Eurasian boreal
 409 flux is masked) runs for 2012 June-August ($3^\circ \times 2^\circ$ spatial resolution). MLO trend from each individual scenario is
 410 removed before the ΔXCO_2 calculation. Same color scale is used as in Fig. 9a. Partial column ΔXCO_2 patterns for
 411 free troposphere (800 to 330 hPa) and lower troposphere (below 800 hPa) are provided in SI.

Formatted: Not Superscript/ Subscript

412 3.5 A comparison with apparent gradients over Europe

413 Figure 11 shows the climatological June - August mean modeled global column ΔXCO_2 map in $3^\circ \times 2^\circ$ spatial
 414 resolution, which presents smooth wave-like patterns. Reuter et al. (2014) use SCIAMACHY and GOSAT satellite
 415 retrievals of column CO_2 and inverse modelling to attain surface CO_2 flux over European region, and suggest a large
 416 uptake of CO_2 in this region. Column ΔXCO_2 from CT2015 (Fig. 11) exhibits a drastically different summer spatial
 417 pattern over Europe compared with the eight year mean (2003-2010) June through August satellite retrievals
 418 presented by Reuter et al. (2014, their Fig. 2a). The spatial gradient from CT2015 results in a maximum 3-4 ppm
 419 difference and a gradual pattern, instead of as much as 6 ppm from satellite retrievals. There is no sign of XCO_2 hot
 420 spots from surface emissions or removals in the CT2015 spatial pattern over Europe (Fig. 11), in contrast to several
 421 hot spots that are apparent from the 8-year averaged SCIAMACHY satellite retrievals over Ireland, U.K., northeast
 422 of France, Belgium, Netherland, north of Germany, and south of Sweden, and low spots over the Ukraine and
 423 Kazakhstan (Reuter et al., 2014). Although the NOAA/ESRL CT2015
 424 (<https://www.esrl.noaa.gov/gmd/ccgg/carbontracker/CT2015/>) assimilates fewer observations over Europe than
 425 Carbon Tracker Europe (<http://www.carbontracker.eu/>), both models produced similar fluxes over the European

426 region (see both websites for detailed fluxes). The $3^\circ \times 2^\circ$ grid from CT2015 is not likely responsible for a much
427 smoother pattern for Carbon Tracker, compared with the $2^\circ \times 2^\circ$ grid from satellite retrievals (Reuter et al., 2014) .
428 The North America region on the $3^\circ \times 2^\circ$ grid in Fig. 11 shows similar pattern as the $1^\circ \times 1^\circ$ grid in Fig. 9, with
429 similar spatial difference of ~ 5 ppm. A smoother spatial distribution should be expected in Europe for the long-term
430 mean column XCO_2 (Fig. 11) due to the influences of dominating west and southwest winds in summer. Since the
431 satellite retrievals in Reuter et al. (2014) appear to show unrealistic column XCO_2 spatial gradients over Europe,
432 they should not be used to derive estimates of a European carbon sink. A recent study (Feng et al., 2016) using
433 inverse modeling suggests that satellite retrievals outside the immediate European region and a small bias of 0.5
434 ppm were sufficient to produce the apparent large carbon sink in the study of Reuter et al. (2014). This is expected
435 from elementary mass balance considerations as in Sec.1. Spatial gradients are the fundamental signals to infer
436 regional fluxes. Since spatial gradients from CT2015 are realistic, boreal fluxes inferred by CT2015, which shows
437 $0.03 \pm 2.33 \text{ Pg C yr}^{-1}$ for Europe, should be more trustworthy than fluxes estimated based on unrealistic spatial
438 pattern. However, the European carbon sink is still inclusive; the discrepancies among different methods and results
439 are further discussed by Reuter et al. (2017). Increasing the amount of highly precise observations such as the well-
440 calibrated surface measurements and vertical profiles can greatly help to estimate the carbon sink.
441
442



443
444 **Fig. 11.** Long-term mean (2004-2014) June - August total column ΔXCO_2 from CT2015 (top panel) in $3^\circ \times 2^\circ$
445 spatial resolution, and zoom-in for Europe overlaid with pressure-weighted (1000 hPa to 500 hPa) mean wind

446 vectors for the same period (bottom panel). The color scale is the same as in Fig. 9a, which is scaled to reflect 6
447 ppm difference of XCO₂ to compare with satellite retrievals from Reuter et al. (their Fig. 2a, 2014).

448 4 Conclusion

449 Aircraft and tall tower measurements from the NOAA GGGRN provide detailed information describing the long-
450 term average temporal and spatial variations of CO₂ in the PBL and the free troposphere. These data provide
451 valuable constraints for evaluating model simulations and satellite retrievals. Seasonal cycle peak-to-peak
452 amplitudes of CO₂ are largest below 2 km, where those maximum values are about twice those in the vertical layers
453 above, indicating that most of the information on surface sources and sinks resides in the continental PBL. Large
454 spatial gradients of CO₂ over North America are observed below 2 km during summer (with maximum difference of
455 ~15.5 ppm between MW and SM), while higher altitude data (above 2 km) have much smaller contributions to
456 spatial gradients, with a maximum difference of ~~only~~ 4 ppm. The spatial differences of CO₂ in the upper troposphere
457 and above (330 hPa to 0 hPa) are less than 0.5 ppm, according to CT2015. Comparison with Aircore measurements
458 shows that the upper troposphere and lower stratospheric simulations from CT2015 are reasonably trustworthy.

459 Our long-term mean vertical profiles show that tower data agree well with aircraft data at similar vertical levels.
460 Partial column ΔXCO₂ was calculated from the long-term mean vertical profiles. By comparing the partial column
461 ΔXCO₂ from measurements with those from CT2015, we verify that CT2015 captures the long-term mean patterns
462 of both phase and amplitude of partial ΔXCO₂.

463 Large spatial gradients of ΔXCO₂ only appeared in summer, during which time the north and northeast regions
464 had ~3 ppm stronger drawdowns than the south and southwest regions. Scattered hot spots of high column ΔXCO₂
465 associated with surface emissions from megacities, or cold spots associated with strong local uptake, are not or just
466 barely visible in the long-term average column ΔXCO₂. Instead, the wave-like pattern of column ΔXCO₂ over North
467 America matches well with large scale circulation. By comparing the spatial gradients of ΔXCO₂ with wind vectors
468 across North America, we find that total column ΔXCO₂ patterns are equally affected by large scale circulation
469 patterns as by regional surface sources and sinks. A CarbonTracker experiment to investigate the impact of Eurasian
470 long-range transport suggests that the large summer time Eurasian boreal flux alone contributes about half of the
471 north-south column ΔXCO₂ gradient across North America. Considering the transported signals from other upwind
472 regions, including northern Canada, we expect that the transported signals overall has major contribution to the
473 column ΔXCO₂ spatial gradient.

Formatted: Not Superscript/ Subscript

474 Author contributions

475 Xin Lan was responsible for study design, data analysis, and manuscript writing. Pieter Tans was responsible for
476 study design, data analysis, and manuscript improvement. Colm Sweeney and Arlyn Andrews provided
477 measurement data and improved manuscript. Andrew Jacobson provided modelled data and improved manuscript.
478 Edward Dlugokencky analyzed measurements and ensured data quality, and improved manuscript. Jonathan Kofler

479 conducted tower measurements and improved manuscript. Molly Crotwell, Patricia Lang, and Sonja Wolter
480 analyzed measurements and ensured data quality. Kirk Thoning provided data smoothing method.

481 **Acknowledgements**

482 We especially thank John Mund for extracting NARR meteorological variables for our measurements. This
483 research was supported by a fellowship from the National Research Council Research Associateship Programs.

484 **References**

- 485 Andrews, A. E., Kofler, J. D., Trudeau, M. E., Williams, J. C., Neff, D. H., Masarie, K. A., Chao, D. Y., Kitzis, D.
486 R., Novelli, P. C., Zhao, C. L., Dlugokencky, E. J., Lang, P. M., Crotwell, M. J., Fischer, M. L., Parker, M. J.,
487 Lee, J. T., Baumann, D. D., Desai, A. R., Stanier, C. O., De Wekker, S. F. J., Wolfe, D. E., Munger, J. W. and
488 Tans, P. P.: CO₂, CO, and CH₄ measurements from tall towers in the NOAA Earth System Research
489 Laboratory's Global Greenhouse Gas Reference Network: instrumentation, uncertainty analysis, and
490 recommendations for future high-accuracy greenhouse gas monitoring efforts, *Atmos. Meas. Tech.*, *7*, 647-687,
491 2014.
- 492 Banta, R. M., Senff, C. J., Nielsen-Gammon, J., Darby, L. S., Ryerson, T. B., Alvarez, R. J., Sandberg, S. R.,
493 Williams, E. J. and Trainer, M.: A bad air day in Houston', *B. Am. Meteorol. Soc.*, *86*, 657, DOI:
494 <http://dx.doi.org/10.1175/BAMS-86-5-657>, 2005.
- 495 Biraud, S. C., Torn, M. S., Smith, J. R., Sweeney, C., Riley, W. J. and Tans, P. P.: A multi-year record of airborne
496 CO₂ observations in the US Southern Great Plains, *Atmos. Meas. Tech.*, *6*, 751-763, 2013.
- 497 Buchwitz, M., Reuter, M., Bovensmann, H., Pillai, D., Heymann, J., Schneising, O., Rozanov, V., Krings, T.,
498 Burrows, J. P., Boesch, H., Gerbig, C., Meijer, Y. and Loscher, A. : Carbon Monitoring Satellite (CarbonSat):
499 assessment of atmospheric CO₂ and CH₄ retrieval errors by error parameterization, *Atmos. Meas. Tech.*, *6*,
500 3477-3500, 2013.
- 501 Chevallier, F., Breon, F. M. and Rayner, P. J.: Contribution of the Orbiting Carbon Observatory to the estimation of
502 CO₂ sources and sinks: Theoretical study in a variational data assimilation framework, *J. Geophys. Res.*
503 *Atmos.*, *112*, D09307, doi:10.1029/2006JD007375, 2007.
- 504 Choi, Y. H., Vay, S. A., Vadrevu, K. P., Soja, A. J., Woo, J. H., Nolf, S. R., Sachse, G. W., Diskin, G. S., Blake, D.
505 R., Blake, N. J., Singh, H. B., Avery, M. A., Fried, A., Pfister, L. and Fuelberg, H. E.: Characteristics of the
506 atmospheric CO₂ signal as observed over the conterminous United States during INTEX-NA, *J. Geophys. Res.*
507 *Atmos.*, *113*, D07301, doi:10.1029/2007JD008899, 2008.
- 508 Ciais, P., Rayner, P., Chevallier, F., Bousquet, P., Logan, M., Peylin, P. and Ramonet, M.: Atmospheric inversions
509 for estimating CO₂ fluxes: methods and perspectives, *Climatic Change*, *103*, 69-92, 2010.
- 510 Conway, T. J., Tans, P. P., Waterman, L. S. and Thoning, K. W.: Evidence for interannual variability of the carbon-
511 cycle from the national-oceanic-and-atmospheric-administration climate-monitoring-and-diagnostics-laboratory
512 global-air-sampling-network, *J. Geophys. Res. Atmos.*, *99*, 22831-22855, 1994.

513 Crevoisier, C., Sweeney, C., Gloor, M., Sarmiento, J. L. and Tans, P. P.: Regional US carbon sinks from three-
514 dimensional atmospheric CO₂ sampling, *Proc. Natl. Acad. Sci. U. S. A.*, 107, 18348-18353, 2010.

515 Crisp, D., Fisher, B. M., O'Dell, C., Frankenberg, C., Basilio, R., Bosch, H., Brown, L. R., Castano, R., Connor, B.,
516 Deutscher, N. M., Eldering, A., Griffith, D., Gunson, M., Kuze, A., Mandrake, L., McDuffie, J.,
517 Messerschmidt, J., Miller, C. E., Morino, I., Natraj, V., Notholt, J., O'Brien, D. M., Oyafuso, F., Polonsky, I.,
518 Robinson, J., Salawitch, R., Sherlock, V., Smyth, M., Suto, H., Taylor, T. E., Thompson, D. R., Wennberg, P.
519 O., Wunch, D., and Yung, Y. L.: The ACOS CO₂ retrieval algorithm – Part II: Global XCO₂ data
520 characterization, *Atmos. Meas. Tech.*, 5, 687–707, doi:10.5194/amt-5-687-2012, 2012.

521 Dee, D. P., Uppala, S. M., Simmons, A. J., Berrisford, P., Poli, P., Kobayashi, S., Andrae, U., Balmaseda, M. A.,
522 Balsamo, G., Bauer, P., Bechtold, P., Beljaars, A. C. M., van de Berg, L., Bidlot, J., Bormann, N., Delsol, C.,
523 Dragani, R., Fuentes, M., Geer, A. J., Haimberger, L., Healy, S. B., Hersbach, H., Holm, E. V., Isaksen, L.,
524 Kallberg, P., Kohler, M., Matricardi, M., McNally, A. P., Monge-Sanz, B. M., Morcrette, J. J., Park, B. K.,
525 Peubey, C., de Rosnay, P., Tavolato, C., Thepaut, J. N. and Vitart, F.: The ERA-Interim reanalysis:
526 configuration and performance of the data assimilation system, *Q.J.R. Meteorol. Soc.*, 137, 553-597, 2011.

527 Denning, A. S., Takahashi, T., and Friedlingstein, P.: Can a strong atmospheric CO₂ rectifier effect be reconciled
528 with a “reasonable” carbon budget?, *Tellus B*, 51, 249–253, 1999.

529 Feng, L., Palmer, P. I., Parker, R. J., Deutscher, N. M., Feist, D. G., Kivi, R., Morino, I. and Sussmann, R.:
530 Estimates of European uptake of CO₂ inferred from GOSAT X-CO₂ retrievals: sensitivity to measurement bias
531 inside and outside Europe, *Atmos. Chem. Phys.*, 16, 1289-1302, 2016.

532 Frankenberg, C., Kulawik, S. S., Wofsy, S., Chevallier, F., Daube, B., Kort, E. A., O'Dell, C., Olsen, E. T., and
533 Osterman, G.: Using airborne HIAPER Pole-to-Pole Observations (HIPPO) to evaluate model and remote
534 sensing estimates of atmospheric carbon dioxide, *Atmos. Chem. Phys.*, 16, 7867–7878, 2016. doi:10.5194/acp-
535 16-7867-2016, 2016.

536 Gerbig, C., Lin, J. C., Wofsy, S. C., Daube, B. C., Andrews, A. E., Stephens, B. B., Bakwin, P. S. and Grainger, C.
537 A.: Toward constraining regional-scale fluxes of CO₂ with atmospheric observations over a continent: 1.
538 Observed spatial variability from airborne platforms *J. Geophys. Res. Atmos.*, 108, doi:10.1029/2002JD003018,
539 2003.

540 [Chevallier, F., Palmer, P. I., Feng, L., Boesch, H., O'Dell, C. W., and Bousquet, P.: Towards robust and consistent](#)
541 [regional CO₂ flux estimates from in situ and space-borne measurements of atmospheric CO₂, *Geophys. Res.*](#)
542 [Lett., 41, 1065–1070, doi:10.1002/2013GL058772, 2014.](#)

543 Gourdji, S. M., Mueller, K. L., Yadav, V., Huntzinger, D. N., Andrews, A. E., Trudeau, M., Petron, G., Nehr Korn,
544 T., Eluszkiewicz, J., Henderson, J., Wen, D., Lin, J., Fischer, M., Sweeney, C. and Michalak, A. M.: North
545 American CO₂ exchange: inter-comparison of modeled estimates with results from a fine-scale atmospheric
546 inversion, *Biogeosci.*, 9, 457-475, 2012

547 Gurney, K. R., Law, R. M., Denning, A. S., Rayner, P. J., Baker, D., Bousquet, P., Bruhwiler, L., Chen, Y. H., Ciais,
548 P., Fan, S., Fung, I. Y., Gloor, M., Heimann, M., Higuchi, K., John, J., Maki, T., Maksyutov, S., Masarie, K.,
549 Peylin, P., Prather, M., Pak, B. C., Randerson, J., Sarmiento, J., Taguchi, S., Takahashi, T. and Yuen, C. W.:

Formatted: Subscript

Formatted: Subscript

550 Towards robust regional estimates of CO₂ sources and sinks using atmospheric transport models, *Nature*,
551 415(6872), 626-630, 2002.

552 Gurney, K. R., Law, R. M., Denning, A. S., Rayner, P. J., Pak, B. C., Baker, D., Bousquet, P., Bruhwiler, L., Chen,
553 Y. H., Ciais, P., Fung, I. Y., Heimann, M., John, J., Maki, T., Maksyutov, S., Peylin, P., Prather, M. and
554 Taguchi, S.: Transcom 3 inversion intercomparison: Model mean results for the estimation of seasonal carbon
555 sources and sinks, *Global Biogeochem. Cycles*, 18, GB1010, doi:10.1029/2003GB002111, 2004.

556 Houweling, S., Breon, F. M., Aben, I., Rodenbeck, C., Gloor, M., Heimann, M. and Ciais, P.: Inverse modeling of
557 CO₂ sources and sinks using satellite data: a synthetic inter-comparison of measurement techniques and their
558 performance as a function of space and time, *Atmos. Chem. Phys.*, 4, 523-538, 2004.

559 Inoue, M., Morino, I., Uchino, O., Miyamoto, Y., Yoshida, Y., Yokota, T., Machida, T., Sawa, Y., Matsueda, H.,
560 Sweeney, C., Tans, P. P., Andrews, A. E., Biraud, S. C., Tanaka, T., Kawakami, S. and Patra, P. K.: Validation
561 of XCO₂ derived from SWIR spectra of GOSAT TANSO-FTS with aircraft measurement data, *Atmos. Chem.*
562 *Phys.*, 13, 9771-9788, 2013.

563 Inoue, M., Morino, I., Uchino, O., Nakatsuru, T., Yoshida, Y., Yokota, T., Wunch, D., Wennberg, P. O., Roehl, C.
564 M., Griffith, D. W. T., Velazco, V. A., Deutscher, N. M., Warneke, T., Notholt, J., Robinson, J., Sherlock, V.,
565 Hase, F., Blumenstock, T., Rettinger, M., Sussmann, R., Kyrö, E., Kivi, R., Shiomi, K., Kawakami, S., De
566 Mazière, M., Arnold, S. G., Feist, D. G., Barrow, E. A., Barney, J., Dubey, M., Schneider, M., Iraci, L.,
567 Podolske, J. R., Hillyard, P., Machida, T., Sawa, Y., Tsuboi, K., Matsueda, H., Sweeney, C., Tans, P. P.,
568 Andrews, A. E., Biraud, S. C., Fukuyama, Y., Pittman, J. V., Kort, E. A., and Tanaka, T.: Bias corrections of
569 GOSAT SWIR XCO₂ and XCH₄ with TCCON data and their evaluation using aircraft measurement data,
570 *Atmos. Meas. Tech.* 9, 3491–3512, 2016, doi:10.5194/amt-9-3491-2016.

571 Karion, A., Sweeney, C., Tans, P., and Newberger, T.: AirCore: An Innovative Atmospheric Sampling System, *J.*
572 *Atmos. Ocean. Tech.*, 27, 1839–1853, doi:10.1175/2010JTECHA1448.1, 2010.

573 Karion, A., C. Sweeney, S. Wolter, T. Newberger, H. Chen, A. Andrews, J. Kofler, D. Neff, and P. Tans (2013),
574 Long-term greenhouse gas measurements from aircraft, *Atmos. Meas. Tech.*, 6(3), 511–526, doi:10.5194/amt-6-
575 511-2013.

576 Keeling, C. D. and Rakestraw, N. W.: The concentration of carbon dioxide in the atmosphere, *J. Geophys. Res.*, 65,
577 2502-2502, 1960.

578 Keppel-Aleks, G., Wennberg, P. O., Washenfelder, R. A., Wunch, D., Schneider, T., Toon, G. C., Andres, R. J.,
579 Blavier, J.-F., Connor, B., Davis, K. J., Desai, A. R., Messerschmidt, J., Notholt, J., Roehl, C. M., Sherlock, V.,
580 Stephens, B. B., Vay, S. A., and Wofsy, S. C.: The imprint of surface fluxes and transport on variations in total
581 column carbon dioxide, *Biogeosci.*, 9, 875– 891, doi:10.5194/bg-9-875-2012, 2012.

582 Kulawik, S. S., Worden, J. R., Wofsy, S. C., Biraud, S. C., Nassar, R., Jones, D. B. A., Olsen, E. T., Jimenez, R.,
583 Park, S., Santoni, G. W., Daube, B. C., Pittman, J. V., Stephens, B. B., Kort, E. A., Osterman, G. B. and Team,
584 T. E. S.: Comparison of improved Aura Tropospheric Emission Spectrometer CO₂ with HIPPO and SGP
585 aircraft profile measurements, *Atmos. Chem. Phys.*, 13, 3205-3225, 2013.

586 Lauvaux, T., Schuh, A. E., Uliasz, M., Richardson, S., Miles, N., Andrews, A. E., Sweeney, C., Diaz, L. I., Martins,
587 D., Shepson, P. B. and Davis, K. J.: Constraining the CO₂ budget of the corn belt: exploring uncertainties from
588 the assumptions in a mesoscale inverse system, *Atmos. Chem. Phys.*, 12, 337-354, 2012.

589 Machida, T., Kita, K., Kondo, Y., Blake, D., Kawakami, S., Inoue, G. and Ogawa, T. : Vertical and meridional
590 distributions of the atmospheric CO₂ mixing ratio between northern midlatitudes and southern subtropics, *J.*
591 *Geophys. Res. Atmos.*, 108(D3), 8401, doi:10.1029/2001JD000910, 2002.

592 Machida, T., Matsueda, H., Sawa, Y., Nakagawa, Y., Hirofani, K., Kondo, N., Goto, K., Nakazawa, T., Ishikawa, K.
593 and Ogawa, T.: Worldwide Measurements of Atmospheric CO₂ and Other Trace Gas Species Using
594 Commercial Airlines, *J. Atmos. Ocean. Tech.*, 25(10), 1744-1754, 2008.

595 Mesinger, F., DiMego, G., Kalnay, E., Mitchell, K., Shafran, P. C., Ebisuzaki, W., Jovic, D., Woollen, J., Rogers,
596 E., Berbery, E. H., Ek, M. B., Fan, Y., Grumbine, R., Higgins, W., Li, H., Lin, Y., Manikin, G., Parrish, D., and
597 Shi, W.: North American regional reanalysis, *B. Am. Meteorol. Soc.*, 87, 343–360, doi:10.1175/BAMS-87-3-
598 343, 2006.

599 Messerschmidt, J., Geibel, M. C., Blumenstock, T., Chen, H., Deutscher, N. M., Engel, A., Feist, D. G., Gerbig, C.,
600 Gisi, M., Hase, F., Katrynski, K., Kolle, O., Lavric, J. V., Notholt, J., Palm, M., Ramonet, M., Rettinger, M.,
601 Schmidt, M., Sussmann, R., Toon, G. C., Truong, F., Warneke, T., Wennberg, P. O., Wunch, D. and Xueref-
602 Remy, I.: Calibration of TCCON column-averaged CO₂: the first aircraft campaign over European TCCON
603 sites, *Atmos. Chem. Phys.*, 11(21), 10765-10777, 2011.

604 Miller, C. E., Crisp, D., DeCola, P. L., Olsen, S. C., Randerson, J. T., Michalak, A. M., Alkhaled, A., Rayner, P.,
605 Jacob, D. J., Suntharalingam, P., Jones, D. B. A., Denning, A. S., Nicholls, M. E., Doney, S. C., Pawson, S.,
606 Boesch, H., Connor, B. J., Fung, I. Y., O'Brien, D., Salawitch, R. J., Sander, S. P., Sen, B., Tans, P., Toon, G.
607 C., Wennberg, P. O., Wofsy, S. C., Yung, Y. L. and Law, R. M.: Precision requirements for space-based X-CO₂
608 data, *J. Geophys. Res. Atmos.*, 112, D10314, doi:10.1029/2006JD007659, 2007.

609 Miller, J. B., Lehman, S. J., Montzka, S. A., Sweeney, C., Miller, B. R., Karion, A., Wolak, C., Dlugokencky, J.,
610 Southon, J., Turnbull, J. C., and Tans, P. P.: Linking emissions of fossil fuel CO₂ and other anthropogenic trace
611 gases using atmospheric ¹⁴CO₂, *J. Geophys. Res.*, 117, D08302, doi:10.1029/2011JD017048, 2012.

612 Miller, S. T. K., Keim, B. D., Talbot, R. W. and Mao, H.: Sea breeze: Structure, forecasting, and impacts, *Rev.*
613 *Geophys.*, 41, 1011, doi:10.1029/2003RG000124, 2003.

614 Miyamoto, Y., Inoue, M., Morino, I., Uchino, O., Yokota, T., Machida, T., Sawa, Y., Matsueda, H., Sweeney, C.,
615 Tans, P. P., Andrews, A. E. and Patra, P. K.: Atmospheric column-averaged mole fractions of carbon dioxide at
616 53 aircraft measurement sites, *Atmos. Chem. Phys.*, 13(10), 5265-5275, 2013.

617 Peters, W., Jacobson, A. R., Sweeney, C., Andrews, A. E., Conway, T. J., Masarie, K., Miller, J. B., Bruhwiler, L.
618 M. P., Petron, G., Hirsch, A. I., Worthy, D. E. J., van der Werf, G. R., Randerson, J. T., Wennberg, P. O., Krol,
619 M. C. and Tans, P. P.: An atmospheric perspective on North American carbon dioxide exchange:
620 CarbonTracker, *Proc. Natl. Acad. Sci. U. S. A.*, 104(48), 18925-18930, 2007.

621 Ramonet, M., Ciais, P., Nepomniachii, I., Sidorov, K., Neubert, R. E. M., Langendorfer, U., Picard, D., Kazan, V.,
622 Biraud, S., Gusti, M., Kolle, O., Schulze, E. D. and Lloyd, J.: Three years of aircraft-based trace gas

623 measurements over the Fyodorovskoye southern taiga forest, 300 km north-west of Moscow, Tellus B-Chem.
624 Phys. Meteor., 54(5), 713-734, 2002.

625 Reuter, M., Bovensmann, H., Buchwitz, M., Burrows, J. P., Connor, B. J., Deutscher, N. M., Griffith, D. W. T.,
626 Heymann, J., Keppel-Aleks, G., Messerschmidt, J., Notholt, J., Petri, C., Robinson, J., Schneising, O., Sherlock,
627 V., Velazco, V., Warneke, T., Wennberg, P. O. and Wunch, D.: Retrieval of atmospheric CO₂ with enhanced
628 accuracy and precision from SCIAMACHY: Validation with FTS measurements and comparison with model
629 results, J. Geophys. Res. Atmos., 116, 2011.

630 Reuter, M., Buchwitz, M., Hilker, M., Heymann, J., Schneising, O., Pillai, D., Bovensmann, H., Burrows, J. P.,
631 Bosch, H., Parker, R., Butz, A., Hasekamp, O., O'Dell, C. W., Yoshida, Y., Gerbig, C., Nehrkom, T.,
632 Deutscher, N. M., Warneke, T., Notholt, J., Hase, F., Kivi, R., Sussmann, R., Machida, T., Matsueda, H. and
633 Sawa, Y.: Satellite-inferred European carbon sink larger than expected, Atmos. Chem. Phys., 14(24), 13739-
634 13753, 2014.

635 [Reuter, M., Buchwitz, M., Hilker, M., Heymann, J., Bovensmann, H., Burrows, J. P., Houweling, S., Liu, Y. Y.,
636 Nassar, F., Chevallier, F., Cias, P., Marshall, J., and Reichstein, M.: How much CO₂ is taken up by the
637 European terrestrial biosphere? Bull. Am. Meteor. Soc., 98, 665–671, doi:10.1175/BAMS-D-15-00310.1, 2017.](#)

638 Saitoh, N., Kimoto, S., Sugimura, R., Imasu, R., Kawakami, S., Shiomi, K., Kuze, A., Machida, T., Sawa, Y. and
639 Matsueda, H.: Algorithm update of the GOSAT/TANSO-FTS thermal infrared CO₂ product (version 1) and
640 validation of the UTLS CO₂ data using CONTRAIL measurements, Atmos. Meas. Tech., 9(5), 2119-2134,
641 2016.

642 Stephens, B. B., Gurney, K. R., Tans, P. P., Sweeney, C., Peters, W., Bruhwiler, L., Ciais, P., Ramonet, M.,
643 Bousquet, P., Nakazawa, T., Aoki, S., Machida, T., Inoue, G., Vinnichenko, N., Lloyd, J., Jordan, A., Heimann,
644 M., Shibistova, O., Langenfelds, R. L., Steele, L. P., Francey, R. J. and Denning, A. S.: Weak northern and
645 strong tropical land carbon uptake from vertical profiles of atmospheric CO₂, Science, 316(5832), 1732-1735,
646 2007.

647 Sweeney, C., Karion, A., Wolter, S., Newberger, T., Guenther, D., Higgs, J. A., Andrews, A. E., Lang, P. M., Neff,
648 D., Dlugokencky, E., Miller, J. B., Montzka, S. A., Miller, B. R., Masarie, K. A., Biraud, S. C., Novelli, P. C.,
649 Crotwell, M., Crotwell, A. M., Thoning, K. and Tans, P. P.: Seasonal climatology of CO₂ across North America
650 from aircraft measurements in the NOAA/ESRL Global Greenhouse Gas Reference Network, J. Geophys. Res.
651 Atmos., 120(10), 5155-5190, 2015.

652 Tanaka, M., Nakazawa, T. and Aoki, S.: Concentration of atmospheric carbon-dioxide over japan, J. Geophys. Res.
653 Ocean., 88(C2), 1339-1344, DOI: 10.1029/JC088iC02p01339, 1983.

654 Tanaka, T., Miyamoto, Y., Morino, I., Machida, T., Nagahama, T., Sawa, Y., Matsueda, H., Wunch, D., Kawakami,
655 S. and Uchino, O.: Aircraft measurements of carbon dioxide and methane for the calibration of ground-based
656 high-resolution Fourier Transform Spectrometers and a comparison to GOSAT data measured over Tsukuba
657 and Moshiri, Atmos. Meas. Tech., 5(8), 2003-2012, 2012.

Formatted: Font: Not Bold

658 Tans, P. P., Conway, T. J. and Nakazawa, T.: Latitudinal distribution of the sources and sinks of atmospheric
659 carbon-dioxide derived from surface observations and an atmospheric transport model, *J. Geophys. Res.*
660 *Atmos.*, 94(D4), 5151-5172, 1989.

661 Tans, P. P., Fung, I. Y. and Takahashi, T.: Observational constraints on the global atmospheric CO₂ budget, *Science*,
662 247(4949), 1431-1438, 1990.

663 Thoning, K. W., Tans, P. P. and Komhyr, W. D.: Atmospheric carbon-dioxide at Mauna Loa observatory. 2.
664 Analysis of the NOAA GMCC data, 1974-1985, *J. Geophys. Res. Atmos.*, 94(D6), 8549-8565, 1989.

665 Washenfelder, R. A., Toon, G. C., Blavier, J. F., Yang, Z., Allen, N. T., Wennberg, P. O., Vay, S. A., Matross, D.
666 M. and Daube, B. C.: Carbon dioxide column abundances at the Wisconsin Tall Tower site, *J. Geophys. Res.*
667 *Atmos.*, 111, D22305, doi:10.1029/2006JD007154, 2006.

668 Wofsy, S. C.: HIPER Pole-to-Pole Observations (HIPPO): finegrained, global-scale measurements of climatically
669 important atmospheric gases and aerosols, *Philos. T. R. Soc. A*, 369, 2073–2086, doi:10.1098/rsta.2010.0313,
670 2011.

671 Wunch, D., Toon, G. C., Wennberg, P. O., Wofsy, S. C., Stephens, B. B., Fischer, M. L., Uchino, O., Abshire, J. B.,
672 Bernath, P., Biraud, S. C., Blavier, J. F. L., Boone, C., Bowman, K. P., Browell, E. V., Campos, T., Connor, B.
673 J., Daube, B. C., Deutscher, N. M., Diao, M., Elkins, J. W., Gerbig, C., Gottlieb, E., Griffith, D. W. T., Hurst,
674 D. F., Jimenez, R., Keppel-Aleks, G., Kort, E. A., Macatangay, R., Machida, T., Matsueda, H., Moore, F.,
675 Morino, I., Park, S., Robinson, J., Roehl, C. M., Sawa, Y., Sherlock, V., Sweeney, C., Tanaka, T. and Zondlo,
676 M. A.: Calibration of the Total Carbon Column Observing Network using aircraft profile data', *Atmos. Meas.*
677 *Tech.*, 3(5), 1351-1362, 2010.

678 [Wunch, D., Wennberg, P. O., Messerschmidt, J., Parazoo, N. C., Toon, G. C., Deutscher, N. M., Keppel-Aleks, G.,](#)
679 [Roehl, C. M., Randerson, J. T., Warneke, T., and Notholt, J.: The covariation of Northern Hemisphere](#)
680 [summertime CO₂ with surface temperature in boreal regions, *Atmos. Chem. Phys.*, 13, 9447–9459,](#)
681 [doi:10.5194/acp-13-9447-2013, 2013.](#)